

---

# Assessing Markov Chain Quality Through Regeneration: Enhancing MCMC Reliability

---

Submitted By

Vishnuprasad Pradeepkumar Reshma

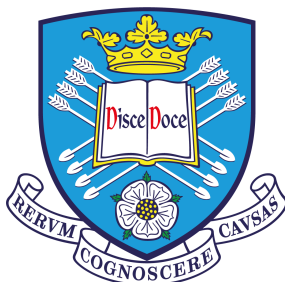
Registration Number: 230164253

Supervisor: Dr. Susan Cartwright

Department of Physics

Submitted in partial fulfilment of the requirements  
of the degree of Master of Science in Particle Physics

August 30, 2024



DEPARTMENT OF PHYSICS  
UNIVERSITY OF SHEFFIELD, UK

## DECLARATION

This dissertation titled “**Assessing Markov Chain Quality Through Regeneration: Enhancing MCMC Reliability**” is the result of my research, except as cited in the references. I have conducted this project under the supervision of **Dr. Susan Cartwright**. This dissertation partially fulfills the requirements for the degree awarded as Master of Science in Particle Physics at the University of Sheffield.

Vishnuprasad Pradeepkumar Reshma

Registration Number: 230164253

30 August 2024

# CONTENTS

<b>List of Figures</b>	<b>4</b>
<b>Acknowledgement</b>	<b>9</b>
<b>Abstract</b>	<b>10</b>
<b>1 Introduction</b>	<b>11</b>
<b>2 Neutrino Physics</b>	<b>14</b>
2.1 Neutrino Discovery .....	14
2.2 Neutrino Oscillation .....	17
2.2.1 Evidence for Neutrino Oscillation .....	17
2.2.2 Theory of Neutrino Oscillation .....	19
2.2.3 The current knowledge of neutrino oscillation parameters.....	22
2.3 Neutrino Interactions .....	23
<b>3 Markov Chain Monte Carlo</b>	<b>24</b>
3.1 Bayesian Inference .....	24
3.2 Monte Carlo (MC) Methods.....	25
3.3 Markov Chain Monte Carlo (MCMC) Method.....	25
3.3.1 Markov chain diagnostics.....	26
3.3.2 Problems of MCMC.....	28
3.4 Summary .....	28
<b>4 Regeneration in MCMC</b>	<b>29</b>
4.1 Regenerative states in a Markov chain.....	29
4.2 Benefits of Regeneration in MCMC.....	30
4.3 Identification of Regeneration states in a Markov chain .....	31
4.3.1 Calculation of the distance from the initial state and middle state...	32
4.4 Diagnostic Methods Using Regeneration .....	33
4.4.1 Variation in the number of regeneration states with the regeneration width (factor) .....	34

4.4.2	Variation in the frequency of steps between regeneration states with the regeneration width .....	34
4.4.3	Variation in the number of entering and leaving regeneration pairs with the regeneration width .....	36
4.4.4	Variation in the frequency of steps between entering and leaving regeneration with the regeneration width.....	36
4.5	Summary .....	38
<b>5</b>	<b>Results: Comparison of Markov chains</b>	<b>39</b>
5.1	Markov chains .....	39
5.2	Comparison of chains with small and large numbers of parameters .....	40
5.2.1	Adaptive fit oscillation chain vs. Asimov chain with adaptation .....	40
5.3	Comparison of chains with and without adaptive step size tuning.....	46
5.3.1	Asimov chain with adaptation vs. Asimov chain without adaptation	46
5.3.2	Adaptive prior-only chain vs. Non-adaptive chain.....	50
5.3.3	Asimov chain with adaptation vs. Non-adaptive chain .....	55
5.3.4	T2K near detector adaptive chain vs. Non-adaptive chain .....	60
5.4	Summary .....	64
<b>6</b>	<b>Conclusions and Outlook</b>	<b>65</b>
<b>References</b>		<b>70</b>

## LIST OF FIGURES

- Figure 3.1:** Trace plot of a well-tuned chain (Page 27)
- Figure 3.2:** Trace plot of a poorly tuned chain (Page 27)
- Figure 3.3:** Markov chain with good autocorrelation plot (Small correlation between successive elements) (Page 27)
- Figure 3.4:** Markov chain with bad autocorrelation plot (Large correlation between successive elements) (Page 27)
- Figure 4.1:** Sample Markov chain with regeneration states (Page 30)
- Figure 4.2:** Factor 0.02 (2% of the total parameter space) represents a small region in the parameter space around the initial state (Page 33)
- Figure 4.3:** Factor 0.3 (30% of the total parameter space) represents a much larger region in the parameter space around the initial state (Page 33)
- Figure 4.4:** Factor 0.02 (2% of the total parameter space) represents a small region in the parameter space around the middle state (Page 33)
- Figure 4.5:** Factor 0.3 (30% of the total parameter space) represents a much larger region in the parameter space around the middle state (Page 33)
- Figure 4.6:** Gradual increase in the number of regenerations with factor represents the chain's well-tuned nature. (Page 34)
- Figure 4.7:** The number of regeneration states is not increasing gradually with factor, representing the poorly tuned nature of the chain. (Page 34)
- Figure 4.8:** The steps between regeneration states dominate in most of the factors, indicating chain's well-repetitive and well-tuned nature (Page 35)
- Figure 4.9:** The steps between regeneration states negligibly small except at factor 0.42, indicating chain's poorly tuned nature (Page 35)
- Figure 4.10:** The presence of large number of entering and leaving pairs indicate the chain's well-tuned nature (Page 36)
- Figure 4.11:** The lack of number of entering and leaving regeneration pairs indicate the chain's poorly tuned nature (Page 36)
- Figure 4.12:** The steps between entering and leaving regeneration states dominate in most of the factors, indicating the chain's well-repetitive and well-tuned nature (Page 37)
- Figure 4.13:** The steps between entering and leaving regeneration states are negligibly small except at factor 0.42, indicating the chain's poorly tuned nature (Page 37)
- Figure 5.1:** Trace and autocorrelation plots of adaptive fit oscillation chain (Page 40)
- Figure 5.2:** Trace and autocorrelation plots of Asimov chain with adaptation (Page 40)

**Figure 5.3:** The comparison of variation in the number of regeneration states with the factor of adaptive fit oscillation chain and Asimov chain with adaptation when the initial state as reference (Page 41)

**Figure 5.4:** The comparison of variation in the number of regeneration states with the factor of adaptive fit oscillation chain and Asimov chain with adaptation when the middle state as reference (Page 41)

**Figure 5.5:** The steps between regeneration states dominate in the adaptive oscillation chain in most of the factors, indicating its well-repetitive and well-tuned nature. Asimov chain has negligible steps between regenerations except at factor 0.42, shows its bad tuning (Reference: Initial state) (Page 42)

**Figure 5.6:** The steps between regeneration states dominate in the adaptive oscillation chain, indicating its well-repetitive and well-tuned nature. Asimov chain has negligible steps between regenerations, shows its bad tuning (Reference: Middle state) (Page 43)

**Figure 5.7:** The steps between entering and leaving regeneration states dominate in the adaptive oscillation chain in most of the factors, indicating its well-repetitive and well-tuned nature. Asimov chain does not leave and enter more often except at factor 0.42, which shows its bad tuning. (Reference: Initial state) (Page 44)

**Figure 5.8:** The steps between entering and leaving regeneration states dominate in the adaptive oscillation chain, indicating its well-repetitive and well-tuned nature. Asimov chain does not leave and enter more often, which shows its bad tuning. (Reference: Middle state) (Page 45)

**Figure 5.9:** Adaptive oscillation chain has a significantly large number of entering and leaving regeneration pairs (Reference: Initial state) (Page 45)

**Figure 5.10:** Adaptive oscillation chain has a significantly large number of entering and leaving regeneration pairs (Reference: Middle state) (Page 45)

**Figure 5.11:** Trace and autocorrelation plots of Asimov chain with adaptation (Page 46)

**Figure 5.12:** Trace and autocorrelation plots of Asimov chain without adaptation (Page 46)

**Figure 5.13:** The comparison of variation in the number of regeneration states with the factor of Asimov chain with and without adaptation when the initial state as reference (Page 47)

**Figure 5.14:** The comparison of variation in the number of regeneration states with the factor of Asimov chain with and without adaptation when the middle state as reference (Page 47)

**Figure 5.15:** Asimov chain without adaptation has a significantly large number of steps between regenerations, indicating the better-tuned nature of this chain (Reference: Initial state) (Page 48)

**Figure 5.16:** Asimov chain without adaptation has a significantly large number of steps between regenerations, indicating the better-tuned nature of this chain (Reference: Middle state) (Page 48)

**Figure 5.17:** Asimov chain without adaptation has a significantly large number of steps between entering and leaving regenerations, indicating the better-tuned nature of this chain (Reference: Initial state) (Page 49)

**Figure 5.18:** Asimov chain without adaptation has a significantly large number of steps between entering and leaving regenerations, indicating the better-tuned nature of this chain (Reference: Middle state) (Page 49)

**Figure 5.19:** Asimov chain without adaptation has a significantly large number of entering and leaving regeneration pairs (Reference: Initial state) (Page 50)

**Figure 5.20:** Asimov chain without adaptation has a significantly large number of entering and leaving regeneration pairs (Reference: Middle state) (Page 50)

**Figure 5.21:** Trace and autocorrelation plots of Adaptive prior-only chain (Page 51)

**Figure 5.22:** Trace and autocorrelation plots of Non-adaptive chain (Page 51)

**Figure 5.23:** The comparison of variation in the number of regeneration states with the factor of adaptive prior-only chain and non- adaptive chain when the initial state as reference (Page 51)

**Figure 5.24:** The comparison of variation in the number of regeneration states with the factor of adaptive prior-only chain and non- adaptive chain when the middle state as reference (Page 51)

**Figure 5.25:** Adaptive prior-only chain has a significantly large number of steps between regenerations, indicating the better-tuned nature of this chain (Reference: Initial state) (Page 52)

**Figure 5.26:** Adaptive prior-only chain has a significantly large number of steps between regenerations, indicating the better-tuned nature of this chain (Reference: Middle state) (Page 53)

**Figure 5.27:** Adaptive prior-only chain has a significantly large number of steps between entering and leaving regenerations, indicating the better-tuned nature of this chain (Reference: Initial state) (Page 53)

**Figure 5.28:** Adaptive prior-only chain has a significantly large number of steps between entering and leaving regenerations, indicating the better-tuned nature of this chain (Reference: Middle state) (Page 54)

**Figure 5.29:** Adaptive prior-only chain has a significantly large number of entering and leaving regeneration pairs (Reference: Initial state) (Page 55)

**Figure 5.30:** Adaptive prior-only chain has a significantly large number of entering and leaving regeneration pairs (Reference: Middle state) (Page 55)

**Figure 5.31:** Trace and autocorrelation plots of Asimov chain with adaptation (Page 55)

**Figure 5.32:** Trace and autocorrelation plots of Non-adaptive chain (Page 55)

**Figure 5.33:** The comparison of variation in the number of regeneration states with the factor of Asimov chain with adaptation and non-adaptive chain when the initial state as reference (Page 56)

**Figure 5.34:** The comparison of variation in the number of regeneration states with the factor of Asimov chain with adaptation and non-adaptive chain when the middle state as reference (Page 56)

**Figure 5.35:** Non-adaptive chain has a significantly large number of steps between regenerations except at factor 0.42, indicating the better-tuned nature of this chain (Reference: Initial state) (Page 57)

**Figure 5.36:** Non-adaptive chain has a significantly large number of steps between regenerations, indicating the better-tuned nature of this chain(Reference: Middle state)(Page 57)

**Figure 5.37:** Non-adaptive chain shows more steps between entering and leaving regenerations except at factor 0.42, indicating the better-tuned nature of this chain (Reference: Initial state) (Page 58)

**Figure 5.38:** The steps between entering and leaving regeneration states dominate in the non-adaptive chain, indicating its well-repetitive and well-tuned nature, which is negligible in the Asimov chain, shows its bad tuning (Reference: Middle state) (Page 59)

**Figure 5.39:** Non-adaptive chain has a significantly large number of entering and leaving regeneration pairs (Reference: Initial state) (Page 60)

**Figure 5.40:** Non-adaptive chain has a significantly large number of entering and leaving regeneration pairs (Reference: Middle state) (Page 60)

**Figure 5.41:** Trace and autocorrelation plots of T2K near detector adaptive chain (Page 61)

**Figure 5.42:** Trace and autocorrelation plots of Non-adaptive chain(Page 61)

**Figure 5.43:** The comparison of variation in the number of regeneration states with the factor of T2K near detector adaptive chain and non-adaptive chain when the initial state as reference(Page 61)

**Figure 5.44:** The comparison of variation in the number of regeneration states with the factor of T2K near detector adaptive chain and non-adaptive chain when the middle state as reference(Page 61)

**Figure 5.45:** The steps between regeneration states dominate in the T2K near detector chain, indicating the chain's well-repetitive and well-tuned nature Reference: Initial state (Reference: Initial state) (Page 62)

**Figure 5.46:** The steps between regeneration states dominate in the T2K near detector chain, indicating the chain's well-repetitive and well-tuned nature Reference: Middle state (Page 62)

**Figure 5.47:** T2K near detector chain has a significantly large number of steps between entering and leaving regeneration states, indicating the better-tuned nature of this chain (Reference: Initial state) (Page 63)

**Figure 5.48:** T2K near detector adaptive chain has a significantly large number of steps between entering and leaving regeneration states, indicating the better-tuned nature of this chain (Reference: Initial state) (Page 63)

**Figure 5.49:** T2K near detector adaptive chain and Non-adaptive chain have a significantly large number of entering and leaving regeneration pairs (Reference: Initial state) (Page 64)

**Figure 5.50:** Non-adaptive chain has a slightly more number of entering and leaving regeneration pairs than the T2K near detector adaptive chain, which is misleading (Page 64)

## ACKNOWLEDGEMENTS

I am deeply indebted to my supervisor, Dr. Susan Cartwright, whose exceptional guidance, encouragement, and support have been the cornerstone of this research. Her profound insights and expertise have been instrumental in shaping both the direction and depth of this dissertation. Her unwavering commitment to excellence and her willingness to offer constructive feedback have significantly enhanced the quality of this work.

I would also like to extend my heartfelt appreciation to Henry Wallace (PhD student) whose patience and willingness to assist me in navigating the intricate world of Markov chains, regeneration techniques, and coding challenges have been invaluable. His expertise and thoughtful advice played a crucial role in helping me overcome the various obstacles encountered during this research. I am especially grateful for his readiness to offer assistance and share his knowledge, which greatly facilitated my progress.

Furthermore, I wish to convey my profound gratitude to my parents. Their unwavering support, both financial and emotional, has been a bedrock of strength throughout my academic journey. Their belief in my abilities and their encouragement have been a constant source of motivation and inspiration.

The completion of this dissertation is a testament to the support and encouragement I have received from these remarkable individuals. I am profoundly grateful for their contributions and cannot thank them enough for their role in this academic endeavor.

**ABSTRACT**

The T2K neutrino oscillation experiment utilizes the Markov chain Monte Carlo (MCMC) method to sample from a probability distribution to estimate neutrino parameters. While MCMC is highly effective for such analysis, it has inherent drawbacks that can impact the identification of best-fit neutrino parameters. Addressing these challenges and ensuring the quality of Markov chains are crucial. Regeneration states within a Markov chain offer a potential solution to some of these issues, providing diagnostic tools to evaluate the chain's behavior. This dissertation explores four critical regeneration diagnostics: the variation in the number of regeneration states with regeneration width, the variation in the frequency of steps between regenerations with regeneration width, the variation in the frequency of steps between entering and leaving regeneration states with regeneration width, and the variation in the number of entering and leaving regeneration pairs with regeneration width. These tools are applied to compare Markov chains with varying parameter counts and those with and without adaptive step-size tuning. Additionally, trace and autocorrelation plots are employed to assess the effectiveness of these diagnostics.

## 1. INTRODUCTION

After discovering neutrino oscillations, it was confirmed that neutrino has mass, which contradicted the Standard Model (SM) prediction, suggesting that a further extension of SM is required. Neutrinos' ability to change their flavor while propagating, aka neutrino oscillation, is characterized by neutrino oscillation parameters such as neutrino mixing angles ( $\theta_{12}$ ,  $\theta_{13}$ ,  $\theta_{23}$ ), mass splitting parameters ( $\Delta m^2_{12}$ ,  $\Delta m^2_{13}$ ,  $\Delta m^2_{32}$ ), and  $\delta_{CP}$  parameter. So, by measuring the neutrino flux change, precise measurements of these parameters can be taken, which can solve many unanswered puzzles in particle physics and cosmology. One puzzle that cosmologists encounter is matter's dominance over antimatter in the Universe. It is believed that matter and antimatter were produced in equal amounts during the Big Bang; however, observations have shown that matter dominates over antimatter. This asymmetry in matter and antimatter is related to charge-parity (CP) symmetry – if CP symmetry is violated, that explains the reason behind the matter dominance over antimatter [1]. Even though CP violation has been observed in quarks [2], it is negligibly small to explain the matter dominance that we observe in this Universe, which makes the study of CP violation in neutrinos significant. The  $\delta_{CP}$  parameter of neutrino oscillation PMNS theory characterizes the considerable violation of CP symmetry in the neutrino sector of the Standard Model. One of the goals of neutrino oscillation experiments like T2K is to measure the best-fit value of this parameter to identify the degree of CP violation in neutrino oscillations. Even though these parameters are crucial to understanding the neutrino oscillation phenomena and PMNS theory, the ambiguity in the sign of  $\Delta m^2_{32}$  parameter leads to two possibilities for the mass ordering: normal ordering  $m_1 < m_2 < m_3$  or inverted ordering  $m_3 < m_1 < m_2$ . So, finding the precise value for the mass splitting parameter, in particular, can improve our understanding of particle physics by explaining the correct ordering of neutrino mass eigenstates. In addition to these neutrino oscillation parameters, neutrino nucleon cross-section parameters strongly impact the neutrino flux measurement, which makes the precise measurements of these parameters significant. T2K deploys a Bayesian statistical approach called the Markov chain Monte Carlo (MCMC) method to identify the precise values of these parameters by fitting the data.

MCMC method is employed in neutrino oscillation experiments primarily for parameter estimation and uncertainty quantification. It is useful to produce samples from the joint

posterior distribution (a combination of the likelihood function and the prior distributions using Bayes' theorem) of the parameters given the observed data, which can be used to find the best-fit values of parameters and uncertainties. Even though MCMC is very efficient in sampling from high-dimensional posterior distributions, it has some drawbacks. Fixing these issues of MCMC is very important to efficiently sample from high dimensional posterior distributions for identifying the best-fit values of parameters. Fortunately, regeneration states in a Markov chain can be very useful in resolving these problems of MCMC.

Regeneration provides solutions to deal the all of the above-mentioned problems of MCMC. Moreover, identifying regeneration states can be a useful diagnostic tool like trace and autocorrelation plots for checking the convergence of a Markov chain. It can be possible to examine whether a chain is well-tuned or not by determining the regeneration states in a Markov chain.

This dissertation focuses on how the identification of regeneration states can be a useful metric for understanding the behavior of Markov chains. To demonstrate that, we consider various convergent and non-convergent chains from the T2K neutrino oscillation analysis group and study how efficient regeneration states are in explaining the convergence property of chains.

Chapter 2 briefly describes neutrinos, which includes the discovery and theory behind neutrino oscillation. Moreover, the current knowledge of neutrino parameters from various oscillation experiments such as solar, reactor, and long baseline is also presented. In addition, a description of neutrino interactions is also presented in this chapter.

The Markov chain Monte Carlo (MCMC) fitting method is a Bayesian analysis, which is useful for neutrino oscillation analysis. A short introduction to Bayesian analysis, MCMC method, various diagnostic methods is presented in Chapter 3.

Chapter 4 presents the soul of this dissertation which explains the regeneration in detail. Moreover, It illustrates various diagnostic methods such as variation in the number of regeneration states with the regeneration width, the variation in the frequency of steps between regeneration states with the regeneration width, the variation in the frequency of steps between entering and leaving regeneration states with the regeneration width, and variation in the number of entering and leaving pairs with the regeneration width, used for analyzing the behavior of chains.

The results obtained from the comparison of various Markov chains with small and large number of parameters and with and without adaptive step size tuning using the four regeneration diagnostic methods are presented in Chapter 5. In addition, it describes how well these diagnostic tools can be good metric to check the convergence of various chains. Chapter 6 summarizes the results of this dissertation.

## 2. NEUTRINO PHYSICS

Observing a continuous energy spectrum of electrons in a beta-decay [3] triggered a vast dilemma in particle physics because this could violate energy conservation in the contemporary understanding of beta decay as a two-body problem. However, in 1930, Wolfgang Pauli [4] proposed a new particle, which is light, neutral, has a  $\frac{1}{2}$  spin, and is somehow not observable to explain this energy spectrum. In 1934, this proposal was theoretically supported by Enrico Fermi's theory of beta-decay [5], in which he gave a new name to this invisible particle: the neutrino. The first observational evidence for this massless particle came from an experiment conducted by Cowan and Reines in 1953 [6] and confirmed in 1956 [7]. However, the idea of being massless from Fermi's theory or Standard Model is contradicted by the observation of neutrino oscillations in SNO [8] and Super-Kamiokande [9] experiments suggest neutrino has mass, even though further studies are required to find the precise values of neutrino mass.

Section 2.1 briefly explains the different neutrino flavors and their discoveries. Section 2.2 introduces the neutrino oscillation phenomenon by explaining various experiments, the theory behind it, and various parameters associated with it. Section 2.3 illustrates the importance of identifying neutrino interactions in a detector.

This dissertation focuses on the quality of various Markov chains, which are used to estimate neutrino oscillation and neutrino interaction parameters, using regeneration.

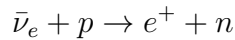
### 2.1 Neutrino Discovery

The theory of Enrico Fermi was a massive success in explaining the beta-decay and predicted that a neutron could decay into a proton, electron, and an anti-neutrino:

$$n \rightarrow p + e^- + \bar{\nu}_e$$

The electrically neutral and negligible mass properties of neutrinos made detecting these particles burdensome; it took more than 20 years to finally detect neutrinos by Reines and Cowan. Due to the small cross-section of neutrinos, many neutrinos are required to make a definite claim of discovery, which is viable only by deploying nuclear reactors. F. Reines and C. L. Cowan detected electron antineutrinos from the inverse beta decay reaction

using two tanks of water placed between liquid scintillators containing 110 photomultiplier tubes (PMTs) positioned near the nuclear reactor [10].

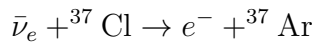


The anti-neutrinos interact with target protons in the water, producing neutrons and positrons. Then, this positron annihilates with an electron in the atom to produce two gamma rays, which create scintillations in the detector and are finally detected by PMTs. The Cadmium in the water, which has a high neutron capture cross-section, enhanced the detection of free neutrons by producing a delayed gamma-ray signal.



The first experimental evidence for the existence of neutrinos came from the delayed gamma-ray signal from the neutron capture and two gamma-ray signals from the annihilation, which substantiated the presence of electron anti-neutrinos [11].

Another experiment by R. Davis [12] demonstrated that anti-neutrinos do not interact to produce electrons, contributing to the formulation of the concept of lepton number conservation. He used carbon tetra chloride to induce inverse beta decay reaction using chlorine expected to produce Argon.



However, the absence of argon atom production suggests the importance of lepton number conservation in a nuclear reaction. Because, lepton number conservation is violated in this reaction which forbids the reaction from happening.

An experiment by L. Lederman, M. Schwartz, J. Steinberger, and collaborators [13] in 1962 explored the possibility of other neutrino flavours by detecting the muon neutrinos and showed that muon neutrinos are coupled to muons just like electron neutrinos couple to electrons, which was confirmed in 1963 at CERN with high-statistics [14]. In this experiment, they used the collision of highly accelerated proton beams with the beryllium target, which produces pions. These pions further decay into muons and anti-muon

neutrinos.

$$\pi^- \rightarrow \mu^- + \bar{\nu}_\mu$$

A spark chamber is used to detect neutrinos by identifying the muons produced by the charged current interaction. Observing an excess of muons than electrons substantiated that muon neutrinos and electron neutrinos are two distinct particles.

The discovery of tau lepton in 1975 [15] by a series of experiments at SLAC using an  $e^+ - e^-$  collider suggested the possibility of a third flavour of neutrino: tau neutrino. The rareness of tau neutrinos and a minimal lifetime of tau leptons ( $2.9 \times 10^{-13}$  s) delayed the discovery of tau neutrinos until the DONUT experiment discovered it [16] in 2000. In this experiment, highly accelerated proton beams (800 GeV) collided with Tungsten, producing an unstable  $D_s$  meson, which decays into tau leptons, which further decays into a tau neutrino. The tau decay was identified using nuclear emulsion detectors by observing the kink in the tau lepton's path, substantiating the tau neutrino's existence. After discovering these neutrinos, the next important question is: Are there any other neutrino flavours we are unaware of? The experiments at the Large Electron Positron (LEP) collider and Standford Linear Accelerator Center (SLAC) by studying the Z boson decays ruled out the possibility of a fourth neutrino flavour. The number of neutrino species  $N_v$  is measured by considering the total decay width of the Z boson mass peak, which is the sum of the visible width, which includes the decays of Z boson into hadrons and leptons, and invisible width, which consists of the decays of Z boson into  $N_v$  neutrino species. The experiment concluded the value of  $N_v$  as  $2.9840 \pm 0.0082$  [17], which was compatible with the idea of three neutrino flavours.

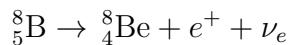
However, the Z boson decay studies do not give a complete picture of the number of neutrino flavours. For instance, many theories proposed the existence of a sterile neutrino that does not take part in weak interaction and could not be studied using Z boson decay channels. Many experiments are looking for sterile neutrinos, but no conclusive evidence has been observed yet. Moreover, heavy neutrino flavours that cannot be produced in Z boson decay might also exist.

## 2.2 Neutrino Oscillation

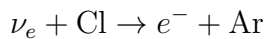
The property of a neutrino to change its flavour as it propagates some distance is defined as neutrino oscillation which is the principal study area of many neutrino experiments such as T2K [18], NOvA [19], etc. In section 2.2.1, the evidence for neutrino oscillation that came from various experiments is presented. The theory behind the neutrino oscillation is explained in section 2.2.2, and the final section, 2.2.3, reviews the current knowledge of neutrino oscillation parameters from various oscillation experiments.

### 2.2.1 Evidence for Neutrino Oscillation

**Solar Neutrinos:** Many experiments focused on detecting highly energetic neutrinos from the  ${}^8\text{B}$  reactions in the Sun.



In 1968, an experiment was designed by Ray Davis and John Bahcall [20] to measure the neutrino flux from this reaction. They used a chlorine liquid ( $\text{C}_2\text{Cl}_4$ ) in the Homestake Mine which provided chlorine atoms to interact with electron neutrinos to produce argon atoms and electrons as given in the equation.



The discrepancy between the number of neutrinos from  ${}^8\text{B}$  reactions using the Standard Solar Model and the number of argon nuclei produced in the experiment caused dilemma. The experiment could only detect one-third of neutrinos than expected from the model, which is called the Solar Neutrino Problem. In 1968, Bruno Pontecorvo [21] proposed an idea suggesting that neutrinos change their flavor as they propagate, called the neutrino oscillation, which causes the deficit in neutrino flux. However, this proposal did not get much attention initially because it contradicted the idea of massless neutrinos predicted by the successful Standard Model theory. The Kamiokande experiment, in 1989, deployed water Cherenkov detectors to identify solar electron neutrinos by detecting the electron recoils from the elastic scattering [22], giving a deficit in neutrino flux that was observed

in the Homestake experiment. In the 1990s, GALLEX [23] and SAGE [24] experiments used Ga to detect solar neutrinos ( $\nu_e + {}^{71}\text{Ga} \rightarrow e^- + {}^{71}\text{Ge}$ ) from the pp chain also agreed with the results from the previous experiments. However, these results were not completely accepted due to the dependence of the inconclusive solar model. Later, the SNO experiment in 2002 [25] measured the solar neutrino flux without relying on the solar model by considering the charged current interaction of electron neutrinos ( $\nu_e + d \rightarrow p + p + e^-$ ) and neutral current interactions of all neutrinos ( $\nu_x + d \rightarrow p + n + \nu_x$ ). The flux of all neutrino flavours observed in the experiment agreed with the predicted value. In contrast, the observed electron neutrino flux showed a discrepancy like in the previous experiments, indicating that electron neutrinos change into muon or tau neutrinos while propagating, which substantiates the neutrino oscillation proposal of Pontecorvo.

**Atmospheric Neutrinos:** Cosmic ray interaction with nuclei in the atmosphere causes the production of muon neutrinos via pion decay.

$$\begin{array}{ll} \pi^+ \rightarrow \mu^+ + \nu_\mu; & \mu^+ \rightarrow e^+ + \nu_e + \bar{\nu}_\mu \\ \pi^- \rightarrow \mu^- + \bar{\nu}_\mu; & \mu^- \rightarrow e^- + \bar{\nu}_e + \nu_\mu \end{array}$$

Reines [26] in 1965 measured the ratio of muon neutrino flux to electron neutrino flux and confirmed that the measured ratio was lower than the predicted values which agreed with the results of IMB [27] and Kamiokande [28] experiments. This problem is called atmospheric neutrino anomaly, but it was not significant enough to ascertain that it was due to neutrino oscillation. However, in 1998, the Super-Kamiokande (SK) experiment measured the flux of upward-going muon neutrinos (travel a large distance) and downward-going muon neutrinos (travel a small distance) and observed a larger deficit in upward-going neutrinos which indicates that muon neutrinos change their flavour while propagating large distance. The observation of disappearing muon neutrinos was solid evidence from the SK experiment to support the neutrino oscillation.

**Reactor Neutrinos:** Various experiments studied neutrinos from nuclear reactors and observed neutrino oscillation by constraining values for oscillation parameters. The KamLAND experiment [29] observed a deficit in the measured muon anti-neutrino flux to the predicted flux, indicating the existence of neutrino oscillation. A similar effect

---

of neutrino oscillation was also observed in other reactor neutrino experiments such as RENO [30], Daya Bay [31], Chooz [32], Double Chooz [33], etc.

**Accelerator Neutrinos:** The control over neutrino energy and baseline distance makes the accelerator neutrino experiments more demanding. These experiments generally deploy high-energy collision of a particle beam with a target to produce meson, which eventually decays into neutrinos. The first accelerator experiment to detect neutrino oscillation using a muon neutrino beam was K2K [34], which was a long baseline (250 km) experiment in Japan. Further evidence came from the observation of muon neutrino disappearance in MINOS [35] agreed with the results of K2K. The observation of tau neutrino appearance in the OPERA [36] experiment in 2010 and electron neutrino appearance in T2K and NOvA experiments further validated the presence of oscillation in the muon neutrino beam.

The plethora of evidence from various experiments supports the theory of neutrino oscillation. However, further studies are required to determine the precise values of neutrino oscillation parameters.

### 2.2.2 Theory of Neutrino Oscillation

According to the Standard Model, the neutrino has three flavour eigenstates: electron neutrino, muon neutrino, and tau neutrino. However, the discovery of neutrino oscillation led to the idea of neutrinos having a mass, introduced new eigenstates called mass eigenstates in addition to the flavour eigenstates of the neutrinos. This means neutrinos have three mass eigenstates with mass  $m_i$  ( $i = 1, 2, 3$ ), and the flavour states can be written as a superposition of these mass eigenstates from the laws of quantum mechanics.

$$|\nu_{\alpha i}| = \sum_i U_{\alpha i}^* |\nu_i|$$

Where  $U$  is called the PMNS (Pontecorvo Maki Nakagawa Sakata) matrix that connects neutrino flavour states with the mass eigenstates. PMNS matrix is  $3 \times 3$  unitary matrix

which takes the form:

$$\begin{bmatrix} U_{e1} & U_{e2} & U_{e3} \\ U_{\mu 1} & U_{\mu 2} & U_{\mu 3} \\ U_{\tau 1} & U_{\tau 2} & U_{\tau 3} \end{bmatrix}$$

where electron neutrino (a flavour state) can be written as  $\nu_e = U_{e1}m_1 + U_{e2}m_2 + U_{e3}m_3$  and a mass state can be written as  $\nu_1 = U_{e1}\nu_e + U_{\mu 1}\nu_\mu + U_{\tau 1}\nu_\tau$ . This PMNS matrix can be parameterised by three mixing angles ( $\theta_{12}, \theta_{13}, \theta_{23}$ ) and the complex phase ( $\delta_{CP}$ ) [37].

$$U = \begin{pmatrix} c_{12}c_{13} & s_{12}c_{13} & s_{13}e^{-i\delta_{CP}} \\ -s_{12}c_{23} - c_{12}s_{23}s_{13}e^{i\delta_{CP}} & c_{12}c_{23} - s_{12}s_{23}s_{13}e^{i\delta_{CP}} & s_{23}c_{13}e^{i\delta_{CP}} \\ s_{12}s_{23} - c_{12}c_{23}s_{13}e^{i\delta_{CP}} & -c_{12}s_{23} - s_{12}c_{23}s_{13}e^{i\delta_{CP}} & c_{23}c_{13}e^{i\delta_{CP}} \end{pmatrix}$$

where  $c_{ij} = \cos \theta_{ij}$  and  $s_{ij} = \sin \theta_{ij}$ . Identifying the best-fit values of these parameters is crucial to determining the PMNS matrix's nature. In a neutrino oscillation experiment, we can not identify the individual masses  $m_1, m_2$ , and  $m_3$  of mass states. However, we can measure the mass-splitting parameters  $\Delta m^2_{12}$ ,  $\Delta m^2_{13}$ , and  $\Delta m^2_{23}$  using neutrino oscillation studies. The critical question is how this neutrino oscillation works. The basic principle of neutrino oscillation is that neutrinos are produced as flavour eigenstates and propagate as mass eigenstates. Consider a neutrino is produced in a flavour state  $\alpha$ ; after travelling some distance  $L$  when it reaches the detector, it will be in another flavour state  $\beta$ , which means that the neutrino changes its flavour during the travel. This phenomenon is called neutrino oscillation. The propagating mass state can be considered as a plane wave

$$|\nu_k(t)\rangle = |\nu_k\rangle e^{i(p_k \cdot x - E_k t)}$$

where  $\nu_k$  is the initial mass state and  $\nu_k(t)$  is the mass state at time  $t$ . We can approximate the speed of neutrino as the speed of light and momentum of neutrino as  $p \approx E(1 - \frac{m^2}{2E^2})$ , which simplifies the exponential to  $e^{-im^2x/2E}$  and the mass state at time  $t$  becomes

$$|\nu_k(t)\rangle = |\nu_k\rangle e^{-im^2x/2E}$$

The main goal of a neutrino oscillation experiment is to identify the probability of transition from one flavour state to another. If we consider the simplest case, the two-

flavour approximation,

$$\begin{pmatrix} \nu_e \\ \nu_\mu \end{pmatrix} = \begin{pmatrix} \cos \theta & \sin \theta \\ -\sin \theta & \cos \theta \end{pmatrix} \begin{pmatrix} \nu_1 \\ \nu_2 \end{pmatrix}$$

electron neutrino and muon neutrino flavour states can be written as  $|\nu_e\rangle = \cos \theta |\nu_1\rangle + \sin \theta |\nu_2\rangle$  and  $|\nu_\mu\rangle = -\sin \theta |\nu_1\rangle + \cos \theta |\nu_2\rangle$  respectively. Suppose that the neutrino is initially at the electron neutrino state  $|\nu_e\rangle$ , after propagating a distance L, the state becomes  $|\nu(L)\rangle$ .

$$\begin{aligned} |\nu(L)\rangle &= \cos \theta |\nu_1\rangle e^{-im_1^2 L/2E_1} + \sin \theta |\nu_2\rangle e^{-im_2^2 L/2E_2}, \\ &= e^{-im_1^2 L/2E_1} (\cos^2 \theta |\nu_e\rangle - \cos \theta \sin \theta |\nu_\mu\rangle) \\ &\quad + e^{-im_2^2 L/2E_2} (\sin^2 \theta |\nu_e\rangle + \cos \theta \sin \theta |\nu_\mu\rangle). \end{aligned}$$

To understand the probability of an electron neutrino transforming into a muon neutrino after travelling a distance of L, we need to find the probability amplitude  $\langle \nu_\mu | \nu(L) \rangle = \cos \theta \sin \theta (e^{-im_2^2 L/2E_2} - e^{-im_1^2 L/2E_1})$  and probability will be the square of this amplitude. After considering  $E_1 = E_2 = E$  and unit conversions, the probability of transition from electron neutrino to muon neutrino:

$$P(\nu_e \rightarrow \nu_\mu) = \sin^2 2\theta \sin^2 \left( \frac{1.27 \Delta m_{21}^2 L}{2E} \right)$$

However, this situation is more complex in three flavour oscillations. For example, the transition probability for muon neutrino to electron neutrino is

$$\begin{aligned} P(\nu_\mu \rightarrow \nu_e) &= 4 \left[ c_{13}^2 s_{12}^2 c_{12}^2 (c_{23}^2 - s_{13}^2 s_{23}^2) + \cos 2\theta_{12} J_r \cos \delta_{CP} \right] \sin^2 \Delta_{21} \\ &\quad + \left[ s_{13}^2 c_{13}^2 c_{12}^2 s_{23}^2 + J_r \cos \delta_{CP} \right] \sin^2 \Delta_{31} \\ &\quad + \left[ s_{13}^2 c_{13}^2 s_{12}^2 s_{23}^2 + J_r \cos \delta_{CP} \right] \sin^2 \Delta_{32} \\ &\quad - J_r \cos \delta_{CP} \sin \Delta_{21} \sin \Delta_{31} \sin \Delta_{32} \end{aligned}$$

where  $c_{ij} = \cos \theta_{ij}$ ,  $s_{ij} = \sin \theta_{ij}$ ,  $\Delta_{ij} = 1.27 \Delta m_{ij}^2 \frac{L}{E}$ ,  $J_r = s_{23} c_{23} s_{13} c_{13}^2 s_{12} c_{12}$  is called the Jarlskog invariant. The survival probability of muon neutrinos in an experiment like

T2K is

$$P(\nu_\mu \rightarrow \nu_\mu) \approx 1 - 4 \cos^2 \theta_{13} \sin^2 \theta_{23} (1 - \cos^2 \theta_{13} \sin^2 \theta_{23}) \sin^2 \frac{\Delta m_{32}^2 L}{4E}$$

So, identifying probabilities for neutrino flavour change can be used to find the precise values of the CP violation parameter ( $\delta_{CP}$ ), neutrino mixing angles ( $\theta_{12}$ ,  $\theta_{13}$ ,  $\theta_{23}$ ), and mass splitting parameters ( $\Delta m_{12}^2$ ,  $\Delta m_{13}^2$ ,  $\Delta m_{32}^2$ ).

### 2.2.3 The current knowledge of neutrino oscillation parameters

The best measurement of  $\theta_{12}$  and  $\Delta m_{12}^2$  come from the combined fit of KamLAND [38] and global solar neutrino data, and they report as  $\sin^2 \theta_{12} = 0.304^{+0.014}_{-0.013}$  and  $\Delta m_{21}^2 = (7.53 \pm 0.18) \times 10^{-5} \text{ eV}^2$ . The high correlation of  $\theta_{23}$  and  $\Delta m_{32}^2$  makes the measurements of these parameters very challenging. However, the best measurement of  $\theta_{23}$  came from T2K depending on the hierarchy of mass states as

$$\sin^2 \theta_{23} = \begin{cases} 0.514^{+0.055}_{-0.056} & (\text{NH}) \\ 0.511^{+0.055}_{-0.055} & (\text{IH}) \end{cases}$$

where NH stands for normal hierarchy ( $m_1 < m_2 < m_3$ ) and IH stands for Inverted Hierarchy ( $m_3 < m_1 < m_2$ ). The best-fit value for  $|\Delta m_{32}^2|$  comes from T2K, MINOS, and Daya Bay as

$$\begin{aligned} |\Delta m_{32}^2| &= (2.42 \pm 0.06) \times 10^{-3} \text{ eV}^2 (\text{NH}) \\ &= (2.49 \pm 0.06) \times 10^{-3} \text{ eV}^2 (\text{IH}) \end{aligned}$$

Moreover, the reactor experiments such as Double Chooz, RENO give the best-fit value for  $\theta_{13}$  as

$$\sin^2 \theta_{13} = (2.19 \pm 0.12) \times 10^{-2}$$

The best results for  $\delta_{CP}$  come from the data of T2K, NOvA, and SK data which suggest the value as

$$\delta_{CP} = 1.37^{+0.18}_{-0.17} \text{ rad (NH)}$$

However, more studies are needed to find the precise values for these oscillation parameters.

### 2.3 Neutrino Interactions

One of the key challenges in measuring neutrino oscillation is the identification of the flux of different neutrino flavours. Understanding neutrino flux, interaction cross-section, detector efficiency, and oscillation probability is vital to identifying the number of neutrinos in the detector. However, in all these components, the low interaction rate of neutrinos constitutes the scarcity of data and a significant increase in the total uncertainty. So, neutrino oscillation studies require a good understanding of cross-section parameters. For example, in an experiment like T2K, we infer the number of neutrinos produced from the decay of mesons, which are generated by the highly energetic collision of protons with the target. So, the only way to identify the presence of different neutrino flavours in a detector is by considering the total number of neutrino interactions happening in the detector. The lack of knowledge of the cross-section parameter creates wrong measurements in the flux of neutrino flavours.

Considering the interactions of neutrinos [39], they can only interact via the weak force, which is mediated by  $W^\pm$  and  $Z^0$  bosons. This weak interaction can be classified based on the exchange particles: The first one is called charged current (CC) interactions, mediated by W bosons, and the second one is called neutral charged (NC) current interactions, mediated by Z bosons. An NC interaction can produce any leptons that are not correlated to the incoming neutrino. Conversely, a CC interaction produces the charged lepton, corresponding to the incoming neutrino's flavour. So, the charged current interaction cross-section measurements are significant for identifying neutrino flavours while NC events are not helpful for oscillation measurements. In the T2K experiment, three CC interactions are essential, and they are quasi-elastic (CCQE), resonance production (CC RES), and deep inelastic scattering (CC DIS), which become dominant based on the neutrino energy. At low energies, CCQE is dominant, which is similar to electron scattering due to the low energy transfer. At intermediate energies, CC RES becomes dominant, which involves the excitation of nuclei into a baryonic resonance and decay, while CC DIS becomes dominant at high energies. Identifying these neutrino interactions is tedious due to the nuclear effects and backgrounds; however, cross-section measurements of these interactions are crucial for neutrino energy reconstruction and oscillation analysis.

### 3. MARKOV CHAIN MONTE CARLO

The experiment uses a Bayesian approach called the Markov chain Monte Carlo (MCMC) method [40] to extract estimates of neutrino oscillation parameters and neutrino cross-section parameters from the T2K data. In this dissertation, the quality of the Markov chains, which consist of oscillation and cross-section parameters, has been assessed. So, it is crucial to have a basic overview of how Markov chains are produced via the MCMC method [41].

This chapter explains the MCMC method, its problems, and various diagnostic techniques. Sections 3.1 and 3.2 briefly describe the general Bayesian approach and Monte Carlo methods. Section 3.3 provides a detailed illustration of the MCMC method, Markov chain diagnostic techniques, and the issues associated with this statistical method.

#### 3.1 Bayesian Inference

One of the critical differences between the Bayesian statistical method and the frequentist approach is how probability is described. In Bayesian inference, probability is the degree of belief or certainty of an event. At the same time, the frequentist approach is based on the frequency of events occurring in repeated sampling or experiments. So, in the Bayesian approach, probability depends on the prior information and changes when new information arrives, while it is irrelevant in the frequentist approach.

The main goal of Bayesian analysis is to produce posterior distribution  $P(\theta | D)$ , which explains the probability of both data D and model parameters  $\theta$  [42]. Using statistical methods, parameter values and uncertainties can be extracted from this posterior distribution, which is the basis of neutrino oscillation analysis. Bayes' theorem [43] is used to construct  $P(\theta | D)$  by giving the relationship between the joint probability distribution  $P(D, \bar{\theta}) = P(D | \bar{\theta}) P(\bar{\theta})$  and posterior distribution.

$$P(\bar{\theta} | D) = \frac{P(D | \bar{\theta}) P(\bar{\theta})}{\int P(D | \bar{\theta}) P(\bar{\theta}) d\bar{\theta}}$$

where  $P(D | \bar{\theta})$  gives the probability of measuring data D given the model parameters  $\theta$  and  $P(\bar{\theta})$  gives the prior distribution which contains all the previous knowledge about the model parameters. The integration used in the equation is not easy to evaluate, so

we can only say  $P(\bar{\theta} | D)$  is proportional to  $P(D | \bar{\theta}) P(\bar{\theta})$  which is sufficient enough to construct posterior distribution  $P(\bar{\theta} | D)$  and extract neutrino parameter estimates.

### 3.2 Monte Carlo (MC) Methods

Monte Carlo methods deploy random sampling to understand a distribution's properties, such as parameter estimates, high-probability regions, and integrals over a distribution. For instance, if we have a high-dimensional, non-analytically solvable integral, a random walk through the parameter space can solve the problem, which is much easier than typical integration.

For instance, if we have to find the area between the two curves, we can use the MC method instead of integration. This method involves scattering random points, identifying the fraction of points within the target region, and multiplying this fraction by the total area of scattered points. This method for finding the area between two curves is highly efficient compared to standard integration. The benefit of the MC method is that we do not need to know the shape of the distribution to find the solution. On the other hand, one of the drawbacks is that this method can give only an approximate solution and requires a large number of random numbers to converge the solution; however, the accuracy of the approximation can be improved by increasing the number of random points. Other vast problems associated with the MC algorithm are its slow convergence and the computational burden. So, many algorithms, such as MCMC, have been developed to tackle these issues.

### 3.3 Markov Chain Monte Carlo (MCMC) Method

The MCMC method is an efficient sampling method that uses Markov chains to sample points from the posterior distribution rather than random sampling. The discrete points are selected by the semi-random walk of the Markov chain through the parameter space, which is more efficient than the standard MC method for high-dimensional parameter spaces.

When a Markov chain moves through the parameter space, each step  $x_i$  of the chain depends only on the previous position  $x_{i-1}$  and is independent of the history of the chain

$(x_0, x_1, \text{etc.})$ . The dimension of the parameter space depends on the number of parameters used in a chain. (This analysis uses various Markov chains of small and large dimensions. Small chains are six-dimensional, which includes only six oscillation parameters, while long chains include many cross-section parameters with dimensions of 145 and 175.)

An essential property of the Markov chain is convergence [44]: after a number of steps, sampling from the chain is the same as randomly taking samples from a particular probability distribution (stationary distribution). By achieving convergence, the chain converges to a stationary distribution, and all the subsequent sample points resemble the samples of that stationary distribution.

To accomplish the convergence, chains must follow three conditions:

**Irreducibility:** The chain must be able to reach any other states in the parameter space by starting from any initial state.

**Recurrence:** After reaching the stationary distribution, the subsequent states must be the samples from the same stationary distribution.

**Aperiodic:** The chain must not be moved periodically in the parameter space.

If the chain follows these three conditions, it will eventually converge to a stationary distribution. However, the number of steps required to achieve convergence varies from chain to chain. Specific diagnostic methods, described in section 3.3.1, can be used to test a chain's convergence. When the chain achieves convergence properly, it can be used to estimate the model parameters  $\theta$ . If the chain does not converge properly, that would lead to misleading estimates, which is why diagnostic techniques are essential.

### 3.3.1 Markov chain diagnostics

MCMC diagnostics [45] are tools used to assess whether the quality of a sample (Markov chain) generated by an MCMC algorithm is adequate for accurately approximating the target distribution. The two diagnostic tools helpful for this study are trace and autocorrelation. The well-behaved trace plot and good autocorrelation plot can indicate a well-tuned Markov chain.

The trace plot shows the sampled values of a parameter as a function of iteration number, which assesses the chain's convergence and mixing. If the chain has converged, the trace plot should display a stable, consistent pattern without noticeable trends or drifts over time, and good mixing is indicated by the chain exploring the parameter space efficiently,

with values varying significantly from one iteration to the next. In contrast, poor mixing is evident when the trace plot shows long stretches of similar values, suggesting the chain gets "stuck" in certain regions. Ideally, a well-behaved trace plot resembles a "fuzzy caterpillar", indicating good convergence and mixing, as shown in Figures 3.1 and 3.2.

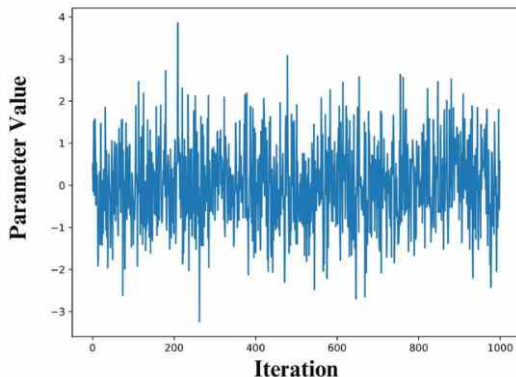


Figure 3.1: Trace plot of a well-tuned chain

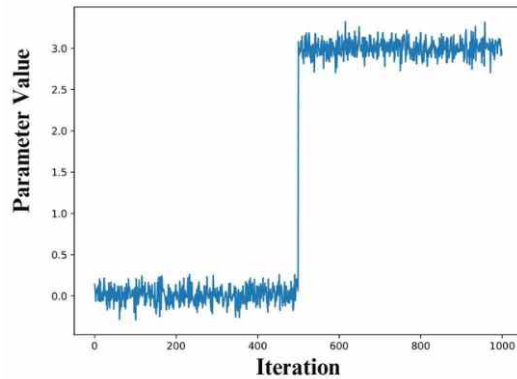


Figure 3.2: Trace plot of a poorly tuned chain

Autocorrelation in Markov Chain Monte Carlo (MCMC) is the correlation between samples taken at different steps in the chain, reflecting how much the current state depends on its previous states. In a good autocorrelation plot, the autocorrelation function (ACF) decreases rapidly and flattens out at zero after a few lags, indicating that the samples become independent quickly. Conversely, a bad autocorrelation plot shows the ACF decreasing slowly, often with oscillations or remaining positive for many lags. This suggests that the chain is not mixing well, leading to highly dependent samples and poor exploration of the parameter space, as shown in Figures 3.3 and 3.4. Nevertheless,

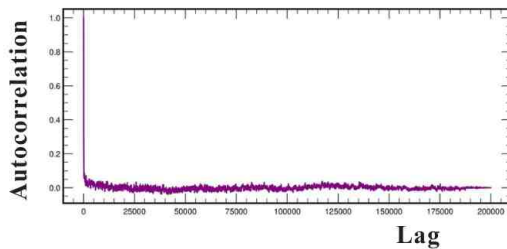


Figure 3.3: Markov chain with a good autocorrelation plot (Small correlation between successive elements)

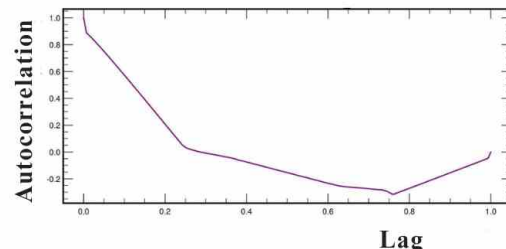


Figure 3.4: Markov chain with a bad autocorrelation plot (Large correlation between successive elements)

it is essential to recognize that no diagnostic tool is without limitations, and we can never be fully confident that an MCMC sample meets the required quality standards.

Although diagnostics can be valuable in detecting potential issues, they cannot eliminate the possibility of errors. Consequently, it is crucial to carefully analyze MCMC samples and employ various diagnostic methods to assess their quality comprehensively.

### 3.3.2 Problems of MCMC

The Markov Chain Monte Carlo (MCMC) method faces several significant challenges. One key issue is the convergence or "burn-in" problem [46], where it's difficult to determine how long it takes for the chain to converge or sufficiently close to its target distribution. Moreover, the requirement of long chains makes the computation using MCMC burdensome. Another issue of MCMC is associated with the difficulty in step size tuning, which is important for the proper mixing of chains; if the step size is small, the chain will be concentrated in a small space and take a huge time to explore the whole parameter space; on the other hand, if the step-size is too high, the chain will often not move.

However, a feature of MCMC is adaptive step size tuning, a technique that automatically adjusts the step size or proposal distribution during sampling, which can solve the chain's mixing problem. This helps the chain converge more quickly to the target distribution by optimizing the step size and reducing the auto-correlation between successive samples, essential for faster convergence and accurate sampling. However, if not implemented correctly, adaptive tuning can introduce dependencies between samples, violating the Markov property and leading to biased results. Identifying and fixing these problems by deploying diagnostic tools mentioned in section 3.3.1 is essential for generating high-quality chains.

## 3.4 Summary

This chapter summarizes the significance of MCMC for finding the best-fit values of neutrino oscillation and cross-section parameters by sampling from a high-dimensional posterior distribution. Moreover, various diagnostic methods and the requirements for more diagnostic tools are described, concluding with problems of MCMC and the relevance of adaptive step size tuning.

## 4. REGENERATION IN MCMC

Identifying regeneration [47] in a Markov chain can be a convenient tool for overcoming some of the issues of MCMC. However, this dissertation focuses on assessing regeneration's ability to introduce new diagnostic tools for Markov chains. For this purpose, various analyses have been done, such as understanding the variation in the number of regeneration states with the regeneration width (factor), the variation in the number of entering and leaving regeneration pairs with the regeneration width, the variation in the frequency of steps between regeneration states with the regeneration width, and the variation in the frequency of steps between entering and leaving regeneration with the regeneration width to check the quality of chains.

This chapter discusses the details of regeneration states in a Markov chain, how it will improve the chain by fixing the problems of Markov chains, and the different diagnostic methods using regeneration.

Section 4.1 illustrates the basic definition of regeneration points (states) and how they can be identified in a Markov chain. The benefits of regeneration state identification are explained in section 4.2, and the method used in the dissertation for identifying regeneration state in a Markov chain is mentioned in section 4.3, while section 4.4 details various diagnostic methods, such as the variation in the number of regeneration states with the regeneration width (factor), the variation in the number of entering and leaving regeneration pairs with the regeneration width, the variation in the frequency of steps between regeneration states with the regeneration width, and the variation in the frequency of steps between entering and leaving regeneration with the regeneration width and how they are valuable tools to check the behavior of chains.

### 4.1 Regenerative states in a Markov chain

A Markov chain is a sequence of possible events or states in a parameter space sampled from a probability distribution using the MCMC method. If the chain restarts or regenerates when it hits a state, we can call it a regeneration state.

The Markov chain in Figure 4.1 shows three states: A, B, and C. Assuming that the chain starts at A, then at B and C, it reaches the same state as A, making B and C as the regeneration states of A (the chain repeats itself at B and C). If we consider a

chain sampled from a high-dimensional parameter space, for instance, a chain with 175 cross-section parameters, a state encompasses the points of 175 parameters, and reaching the same state with the same parameter values to achieve regeneration can be difficult.

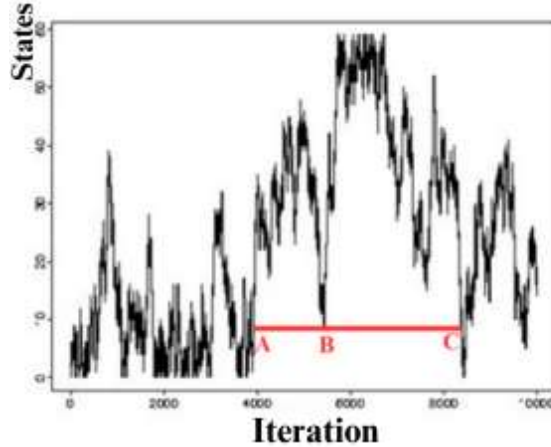


Figure 4.1: Sample Markov chain with regeneration states

In this analysis, various Markov chains—chains with small and large numbers of parameters, for example, an oscillation chain consists of only six oscillation parameters, cross-section chains comprised of 175 or 145 cross-section parameters, and chains with and without adaptive step-size tuning—are considered.

## 4.2 Benefits of Regeneration in MCMC

Regenerative simulation can solve many MCMC problems, as mentioned in section 3.3.2. For example, regenerative simulation can avoid the burn-in problem [48] by providing consistent estimates of estimators' variance. The tours between regenerations are independent and identically distributed (iid), so the presence of regeneration points indicates that the chain has forgotten its initial state and has reached a state typical of the stationary distribution [49]. This helps identify when the burn-in period is over, as samples collected after a regeneration state are more likely to be from a stationary distribution. So, we can discard all the samples up to the first regeneration point, which effectively removes the burn-in period [50]. Moreover, adaptive schemes can be quickly introduced into MCMC using regeneration, which can improve the mixing of chains. Because Markov chains naturally split at regeneration points, anything that happens at these points does not count. So, we can modify the proposal function, which improves the

mixing of chains. Furthermore, the tours between the regeneration can be generated using multiple processors and patched together instead of using a single processor [51], which reduces the computational burden of MCMC. In summary, regeneration can significantly enhance the properties of Markov chains, highlighting the critical need for further research in this area.

In addition to these benefits, identifying regeneration can be a valuable method for understanding the behavior of Markov chains. This diagnostic method can help us check the quality of chains, which is important for measuring the neutrino parameters precisely.

### 4.3 Identification of Regeneration states in a Markov chain

A Markov chain is usually very long and has many states or points. Identifying regeneration states that exist in a small fraction of total parameter space and how they change with the gradual increase of considered space is essential to assess the quality of chains. Two approaches are considered for exploring the parameter space in regeneration state identification: one uses the initial state as a reference point, while the other uses the middle state as a reference point, as discussed in section 4.3.1. However, the relevant question is how we can identify the regenerative states. A method called the spherical approach is introduced, which uses the Euclidean metric to determine whether a state is regenerative or not. According to this method, let's assume the initial state (middle state) as a reference point if the Euclidean distance between the initial state (middle state) and the next state is smaller than the radius or distance threshold around the initial state (middle state); we can conclude that the next state is a regeneration state.

To be precise, if we have a state  $[z_1, z_2, z_3, z_4, z_5, z_6]$  for six parameters and want to check whether it's a regeneration state, let's assume the initial state (middle state) is  $[y_1, y_2, y_3, y_4, y_5, y_6]$  and the distance of these parameters from the initial state (middle state) is  $[x_1, x_2, x_3, x_4, x_5, x_6]$ .

If the Euclidean metric

$$\begin{aligned} & \sqrt{(y_1 - z_1)^2 + (y_2 - z_2)^2 + (y_3 - z_3)^2 + (y_4 - z_4)^2 + (y_5 - z_5)^2 + (y_6 - z_6)^2} \\ & \leq \sqrt{(x_1)^2 + (x_2)^2 + (x_3)^2 + (x_4)^2 + (x_5)^2 + (x_6)^2} \end{aligned}$$

condition is satisfied, then we can say that the state  $[z_1, z_2, z_3, z_4, z_5, z_6]$  is a regeneration state.

#### 4.3.1 Calculation of the distance from the initial state and middle state

The two main strategies to assess the quality of chains are to look for patterns suggesting how often the chain is regenerating or repeating with the distance from the initial state and middle state. To achieve this, firstly, we should consider a small spherical region with a center as the initial state (middle state) and a radius as the distance from the initial state (middle state); then, we have to identify the regeneration states in that small region of the parameter space and by gradually increasing the distance or fraction of total parameter space for regeneration state identification can help understand the chain's behavior.

To measure the distance from the reference point (initial or middle state), first, take the reference point of a single parameter  $n$  in a long Markov chain; the maximum and minimum values it reaches are  $I_{max}$  and  $I_{min}$ , respectively. Using these parameter values, we can find the point furthest from point  $n$ , and the maximum search range would be  $[n-L, n+L]$ .

Consider a small range, say 2% of the total range. It will be  $[n-0.02*L, n+0.02*L]$ , corresponding to that single parameter's distance from the reference point (regeneration width). The same procedure must be followed for a six-dimensional chain with six parameters to find the distance from the reference point for all the parameters and identify the regeneration states in this small range. Then, regeneration width can be increased by considering 4% of the total range, which is  $[n-0.04*L, n+0.04*L]$ , and the regeneration states in this region can be identified. Repeat this procedure by increasing the step size, such as 6%, 8%, etc., until it covers the whole range (100%), and identify regeneration states for each range using the Euclidean approach.

For example, two Markov chains with different ranges in the initial and middle reference states are given in figures 4.2, 4.3, 4.4, and 4.5. Identifying the regeneration states in each of these factors can explain how well-tuned a Markov chain is.

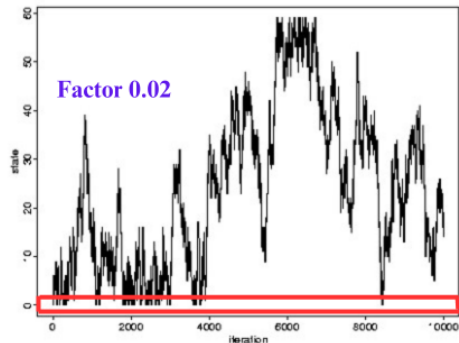


Figure 4.2: Factor 0.02 (2% of the total parameter space) represents a small region in the parameter space around the **initial state**

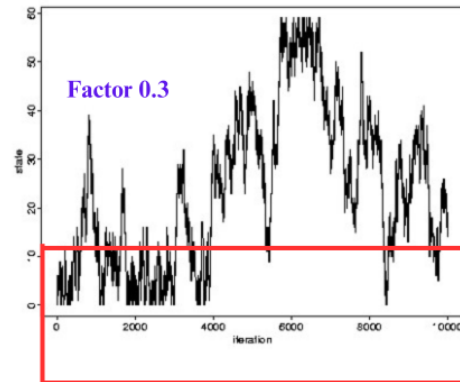


Figure 4.3: Factor 0.3 (30% of the total parameter space) represents a much larger region in the parameter space around the **initial state**

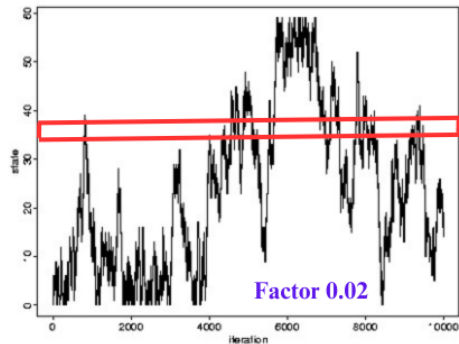


Figure 4.4: Factor 0.02 (2% of the total parameter space) represents a small region in the parameter space around the **middle state**

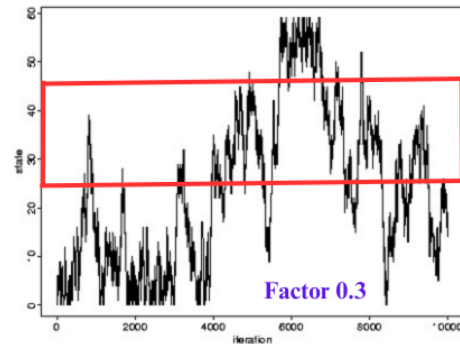


Figure 4.5: Factor 0.3 (30% of the total parameter space) represents a much larger region in the parameter space around the **middle state**

#### 4.4 Diagnostic Methods Using Regeneration

Four analysis tools can be deployed using the regeneration states to study the behavior of Markov chains, such as

- 1) The variation in the number of regeneration states with the regeneration width (factor)
- 2) The variation in the frequency of steps between regeneration states with the regeneration width
- 3) The variation in the number of entering and leaving regeneration pairs with the regeneration width
- 4) The variation in the frequency of steps between entering and leaving regeneration with the regeneration width

#### 4.4.1 Variation in the number of regeneration states with the regeneration width (factor)

Identification of regeneration states and their variation with the increase in the regeneration width can be a handy tool for checking whether a chain is repeating. If a chain consists of more regeneration states, that does not suggest that the chain is repeating, converging, and better tuned because it may indicate a chain that is not leaving and getting stuck in a state. The smooth increase in the number of regenerations with factor indicates a well-behaved chain's repeating and converging nature (Figure 4.6). On the other hand, if the chain shows fluctuations or non-smoothness, it suggests that the chain is not repeating enough and not converging, giving a poorly tuned chain (Figure 4.7).

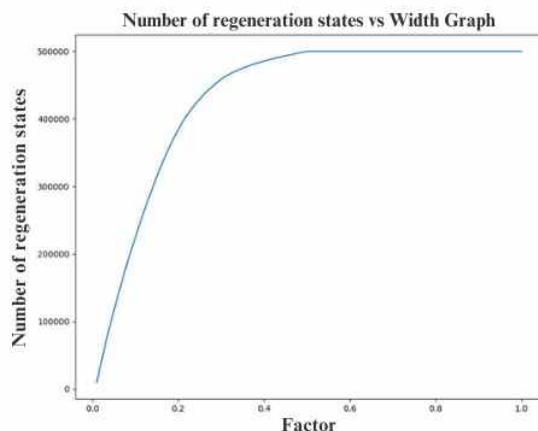


Figure 4.6: Gradual increase in the number of regenerations with factor represents the chain's well-tuned nature.

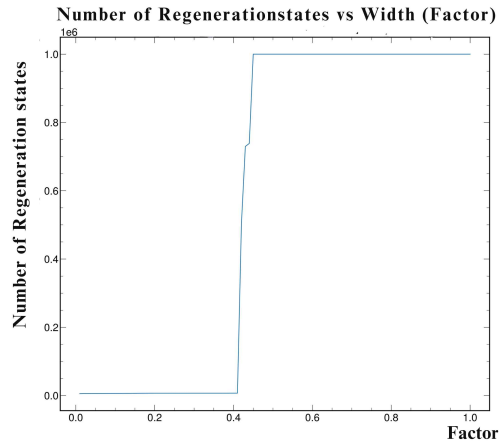


Figure 4.7: The number of regeneration states is not increasing gradually with factor, representing the poorly tuned nature of the chain.

#### 4.4.2 Variation in the frequency of steps between regeneration states with the regeneration width

Identifying the pattern in the steps between regeneration states and how it changes with the increase in regeneration width can be a useful metric for assessing the quality of chains. If a chain shows many steps between regenerations, it can indicate that the chain is repeating, regenerating more often, resulting in a well-tuned chain (Figure 4.8). On the other hand, if a chain shows very few steps between regeneration, it can indicate that the chain is not repeating, resulting in a poorly tuned chain (Figure 4.9).

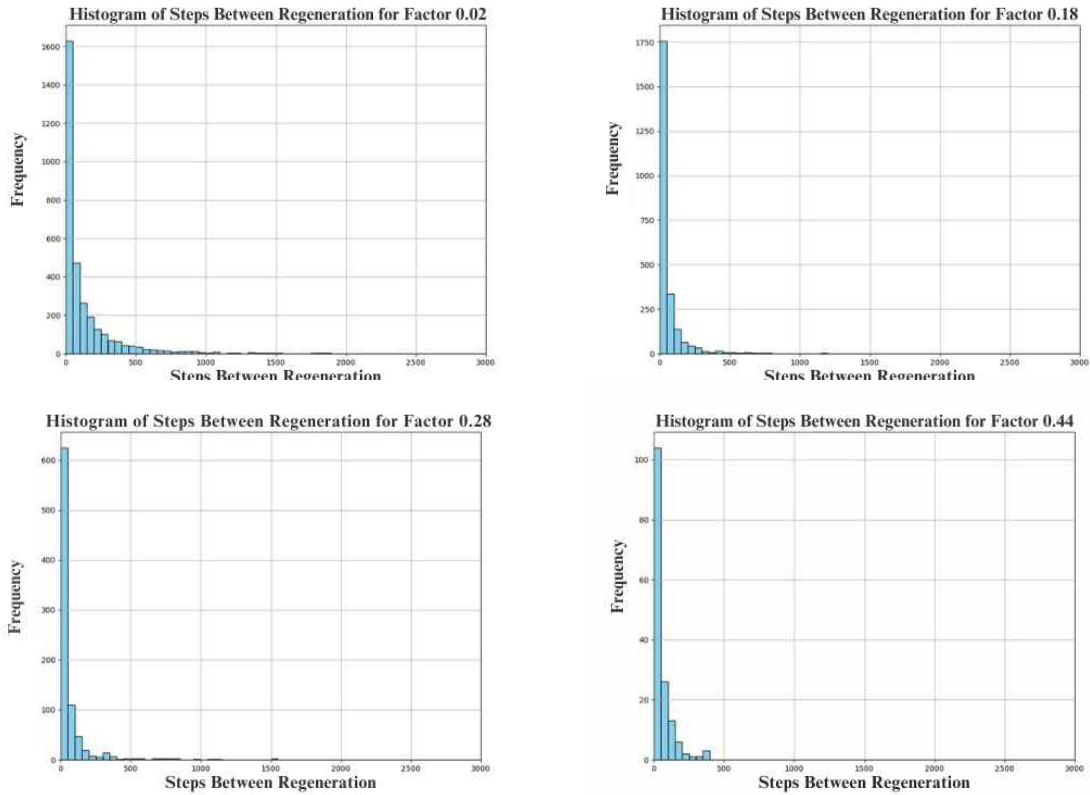


Figure 4.8: The steps between regeneration states dominate in most of the factors, indicating chain's well-repetitive and well-tuned nature

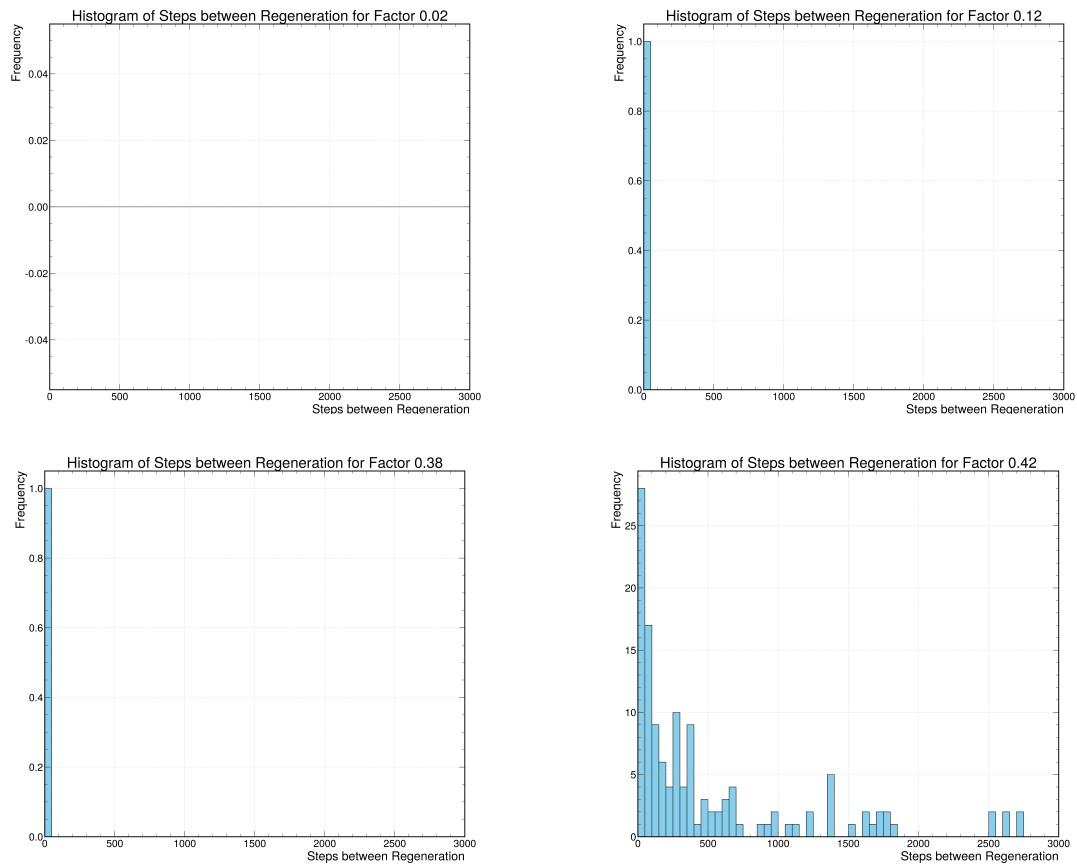


Figure 4.9: The steps between regeneration states negligibly small except at factor 0.42, indicating chain's poorly tuned nature

#### 4.4.3 Variation in the number of entering and leaving regeneration pairs with the regeneration width

Another tool for assessing the chain is identifying the number of entering and leaving regeneration pairs with the regeneration width. For example, if a chain has more entering and leaving pairs, it can indicate that it is leaving and entering the regeneration more often, which signifies a well-tuned nature (Figure 4.10). On the other hand, if the chain has very few entering and leaving pairs with an increase in regeneration width, it indicates the behavior of a poorly tuned chain (Figure 4.11).

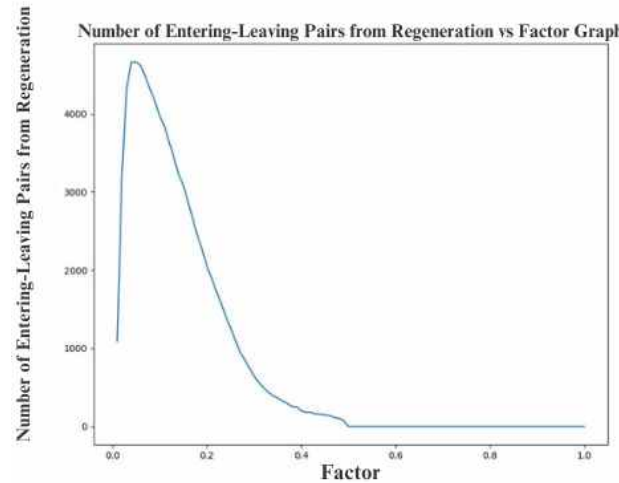


Figure 4.10: The presence of large number of entering and leaving pairs indicate the chain's well-tuned nature

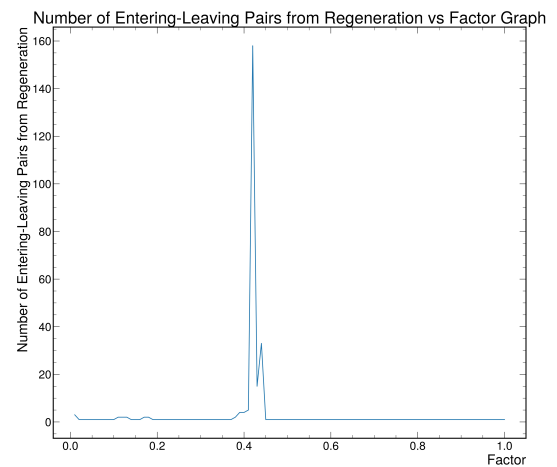


Figure 4.11: The lack of number of entering and leaving regeneration pairs indicate the chain's poorly tuned nature

#### 4.4.4 Variation in the frequency of steps between entering and leaving regeneration with the regeneration width

Identifying the steps between entering and leaving regeneration and understanding their variation with the regeneration width can be a handy tool for checking whether a chain is well-tuned. For instance, if the chain enters and leaves regeneration more often, it is well-tuned (Figure 4.12). On the contrary, if the chain is not entering and leaving regeneration more often, it can indicate a poorly tuned chain (Figure 4.13).

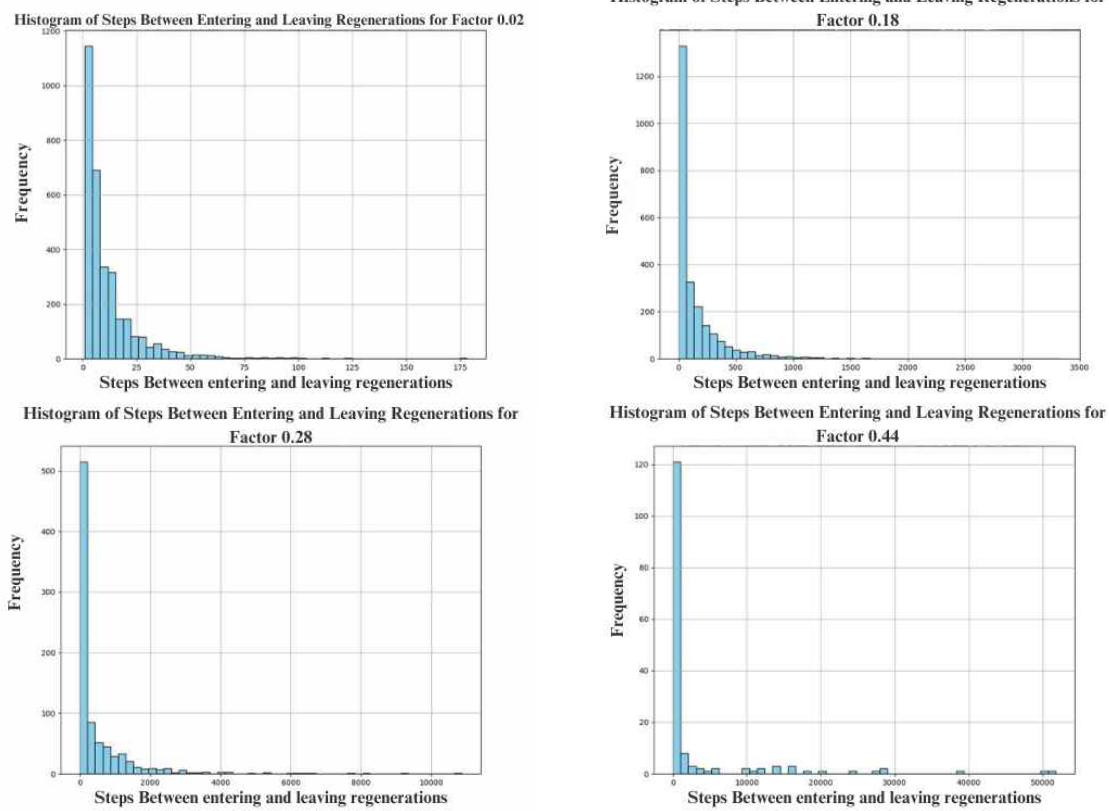


Figure 4.12: The steps between entering and leaving regeneration states dominate in most of the factors, indicating the chain's well-repetitive and well-tuned nature

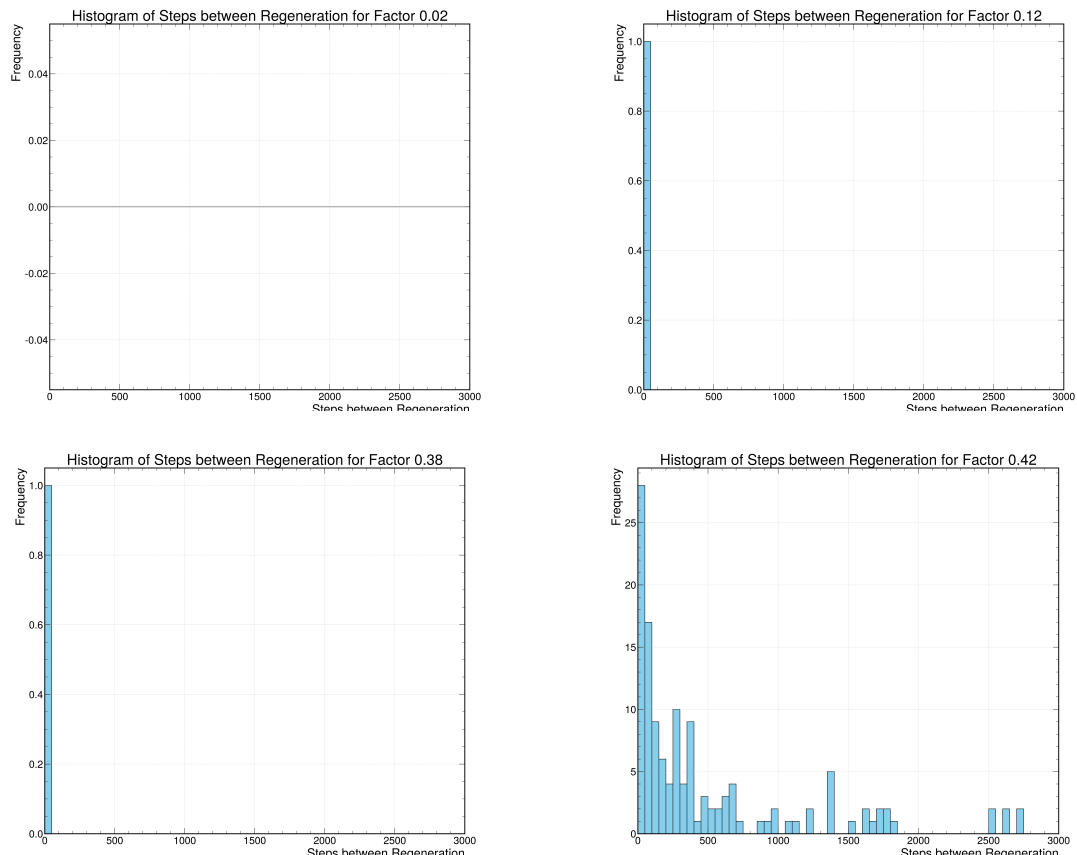


Figure 4.13: The steps between entering and leaving regeneration states are negligibly small except at factor 0.42, indicating the chain's poorly tuned nature

#### 4.5 Summary

This chapter summarizes the significance of regeneration in a Markov chain and how it fixes the issues of MCMC. Moreover, the method used to identify regeneration states and various new diagnostic methods, which can effectively reveal the nature of a chain, are presented.

## 5. RESULTS: COMPARISON OF MARKOV CHAINS

This section details the results of comparing various Markov chains of a large number of parameters with and without adaptive step size tuning using the four analysis tools, ‘The number of regeneration states vs. regeneration width (factor)’, ‘The frequency vs. steps between regeneration for factors’, ‘The number of entering and leaving regeneration pairs vs. regeneration width,’ and ‘The frequency vs. steps between entering and leaving regeneration width for factors’ by considering both the distance from the initial state and the distance from the middle state as references.

Section 5.1 illustrates a brief overview of various Markov chains deployed for comparison. Section 5.2 compares chains with small and large numbers of parameters to demonstrate how well regeneration diagnostic methods work. Section 5.3 compares chains of many parameters with and without adaptive step size tuning and section 5.4 summarizes the main findings observed in the analysis using these diagnostic tools.

### 5.1 Markov chains

For this analysis, various Markov chains with different characteristics were considered, including chains with small and large numbers of parameters and chains with and without adaptive step size tuning. The smallest chain used for comparison is a well-tuned neutrino oscillation chain, consisting of six parameters ( $\theta_{12}$ ,  $\theta_{13}$ ,  $\theta_{23}$ ,  $\Delta m^2_{12}$ ,  $\Delta m^2_{23}$ , and  $\delta_{CP}$ ) with adaptive step size tuning enabled, referred to as the ‘adaptive fit oscillation chain’.

Additionally, several cross-section chains with numerous neutrino cross-section parameters were analyzed. These include both chains with step-size adaptation and those without. Among them are Asimov chains, derived from fitting simulated Monte Carlo data, which include chains both with and without adaptation. Other chains considered are the T2K near detector adaptive chain, an adaptive prior-only chain (flat or Gaussian), and a non-adaptive cross-section chain. The Asimov and T2K near detector adaptive chains each have 175 cross-section parameters, whereas the adaptive prior-only chain and the non-adaptive cross-section chain each have 145 cross-section parameters.

## 5.2 Comparison of chains with small and large numbers of parameters

This section compares an oscillation chain with only six parameters, the 'adaptive fit oscillation chain,' and a cross-section chain with 175 cross-section parameters, the 'Asimov chain with adaptation'. If a chain has a small number of parameters, it is more likely to repeat the states and converge; conversely, a chain with many parameters is less likely to repeat and converge properly. So, a chain with a few parameters is highly well-tuned; comparing it with a poorly tuned chain with many parameters is an easy way to show that regeneration diagnostic methods work for assessing the quality of chains.

### 5.2.1 Adaptive fit oscillation chain vs. Asimov chain with adaptation

By looking at the trace and autocorrelation plots of the two chains, it is evident that the  $\delta_{CP}$  parameter of the adaptive fit oscillation chain (Figure 5.1) explores the parameter space many times and shows a negligible correlation between successive elements, indicating that this is a well-tuned chain. On the other hand, the cross-section parameter of the Asimov chain with adaptation (Figure 5.2) does not explore the parameter space (the trace plot is nearly flat in the middle), and successive elements are highly correlated, suggesting that this is a poorly tuned chain.

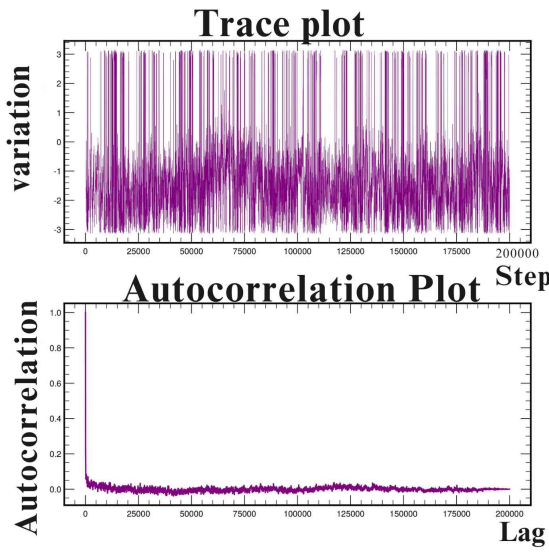


Figure 5.1: Trace and autocorrelation plots of adaptive fit oscillation chain

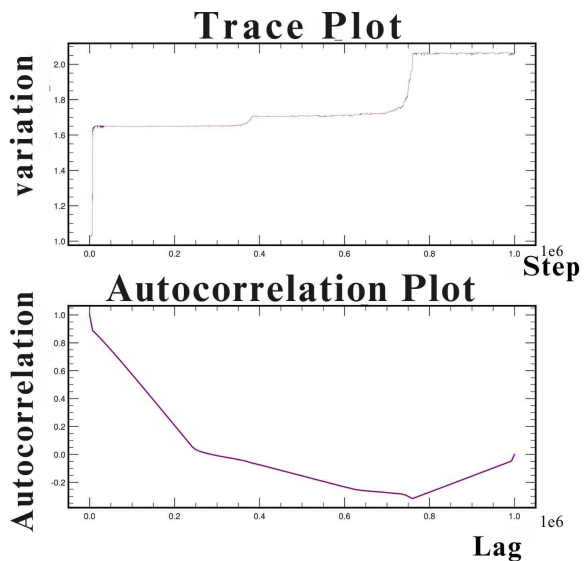


Figure 5.2: Trace and autocorrelation plots of Asimov chain with adaptation

The number of regeneration states in the adaptive fit oscillation chain, obtained by considering the initial state as the reference point (Figure 5.3), shows a smooth increase with the regeneration width, which indicates that this is a well-tuned chain. In the Asimov chain with adaptation, the number of regeneration states does not increase initially; instead, it remains constant until factor 0.4 and increases significantly from factor 0.42 to 0.46. This unsmooth nature of the curve of the Asimov chain is an explicit demonstration of a poorly tuned behavior. In the case of the middle state as a reference (Figure 5.4), the Asimov chain shows many more regeneration states than the oscillation chain. By looking at the trace plot, it is evident that the Asimov chain is flat (constant) in the middle part, indicating a significant increase in the number of regenerations with factor. Still, non-smoothness in the number of regeneration states vs. factor graph demonstrates this chain's non-repetitive behavior and poorly tuned nature.

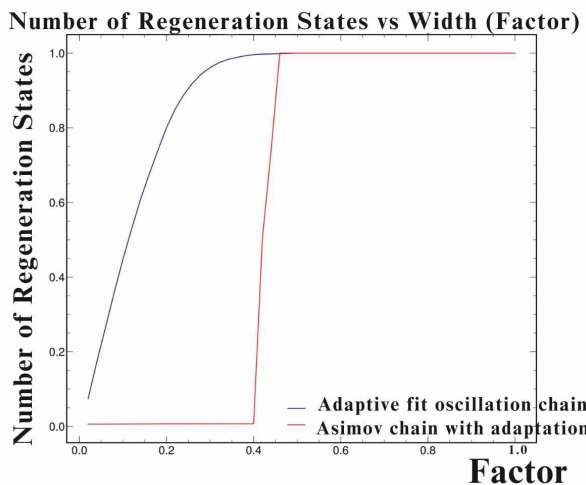


Figure 5.3: The comparison of variation in the number of regeneration states with the factor of adaptive fit oscillation chain and Asimov chain with adaptation when the **initial state as reference**

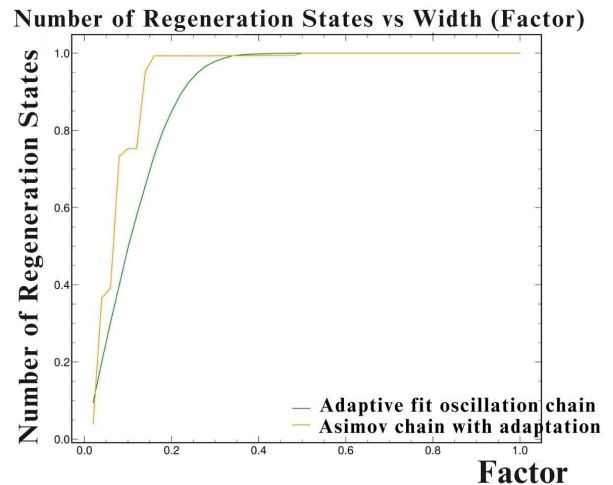


Figure 5.4: The comparison of variation in the number of regeneration states with the factor of adaptive fit oscillation chain and Asimov chain with adaptation when the **middle state as reference**

The variation in the frequency of steps between regeneration with the regeneration width as initial state as reference (Figure 5.5) portrays that the adaptive fit oscillation chain shows more steps between regenerations in smaller regeneration width and decreases eventually, suggesting that this chain repeats more often, stipulating a well-tuned nature. In contrast, in the case of the Asimov fit with adaptation chain, which does not show steps between regenerations initially indicates that this chain is not repeating (evident

from the trace plot), a clear indication of a poorly tuned chain. However, considering the overall steps between regenerations, which are substantial for the adaptive fit oscillation chain compared to the Asimov fit with adaptation except at factor 0.42. In the case of the middle state as a reference (Figure 5.6), the adaptive oscillation chain shows more steps between regenerations (well-tuned), as we expected. In contrast, the other indicates few steps between regenerations (not well-tuned).

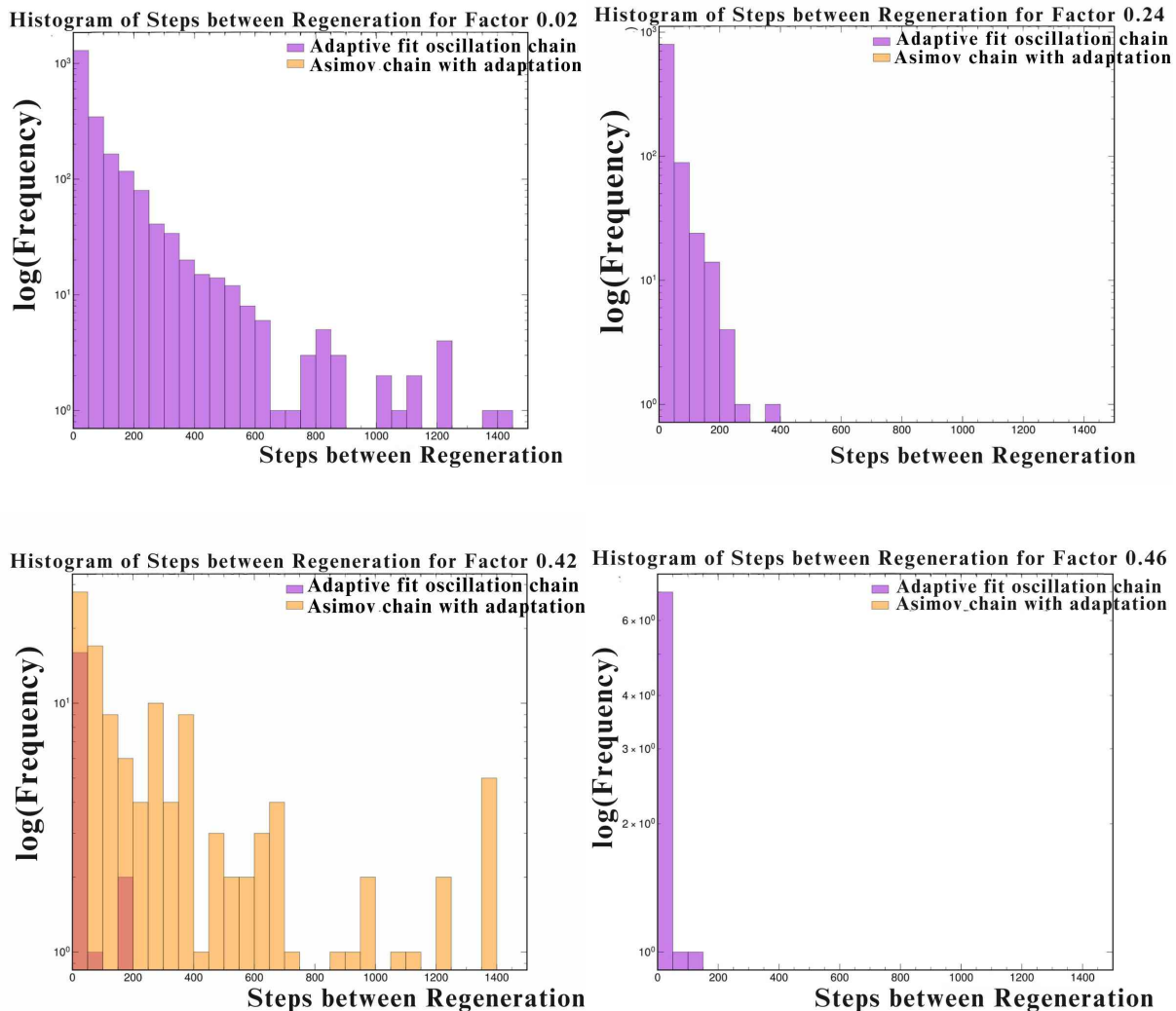


Figure 5.5: The steps between regeneration states dominate in the adaptive oscillation chain in most of the factors, indicating its well-repetitive and well-tuned nature. Asimov chain has negligible steps between regenerations except at factor 0.42, shows its bad tuning (**Reference: Initial state**)

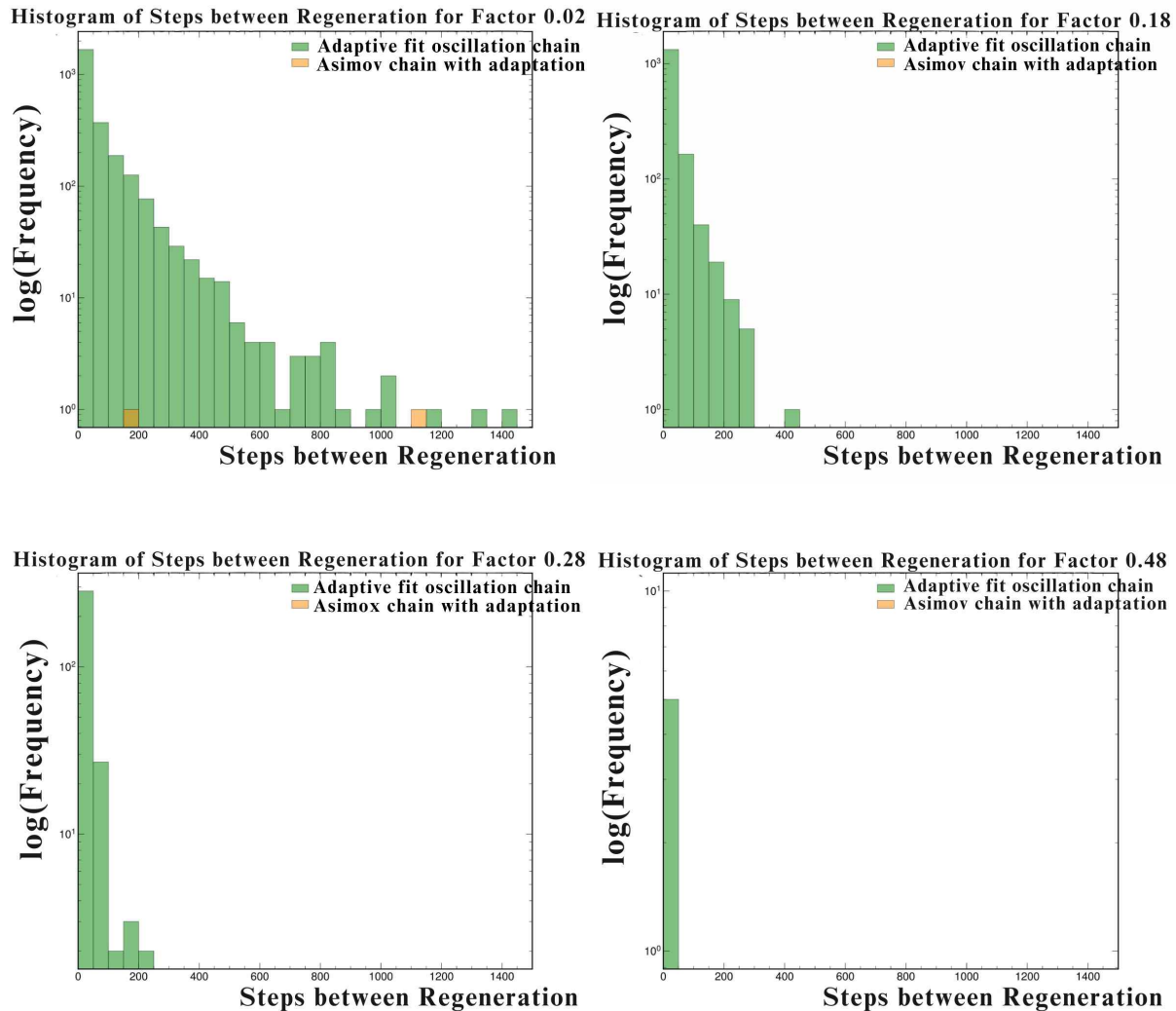


Figure 5.6: The steps between regeneration states dominate in the adaptive oscillation chain, indicating its well-repetitive and well-tuned nature. Asimov chain has negligible steps between regenerations, shows its bad tuning (**Reference: Middle state**)

The variation in the frequency of steps between entering and leaving regeneration with the regeneration width as the initial state as reference (Figure 5.7) illustrates that the adaptive fit oscillation chain is leaving and entering the regeneration more often for a smaller regeneration width, while the Asimov fit with adaptation chain is not leaving and entering the regeneration much except at factor 0.42, which indicates the well-tuned nature of oscillation chain and poor nature of cross-section chain.

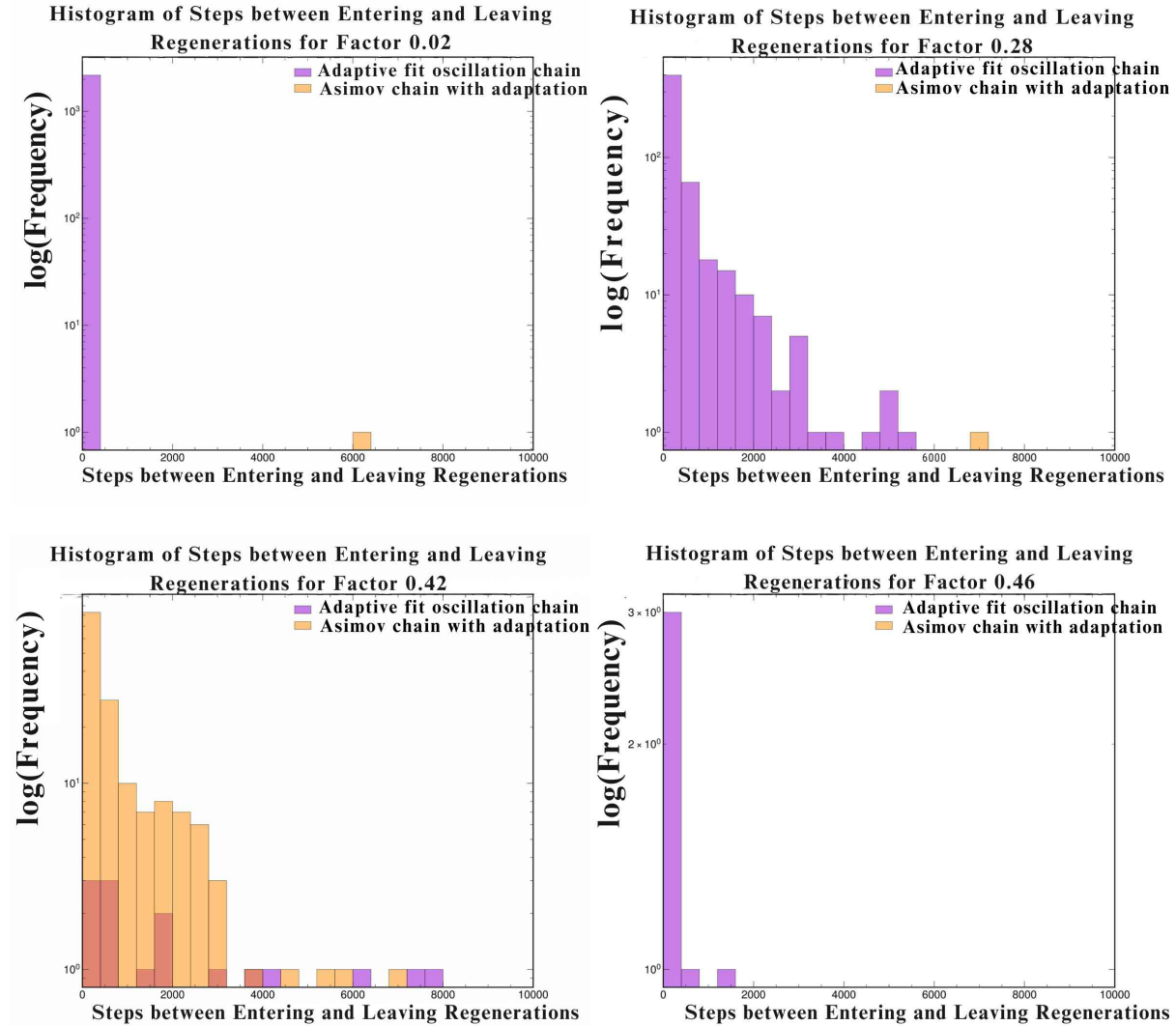


Figure 5.7: The steps between entering and leaving regeneration states dominate in the adaptive oscillation chain in most of the factors, indicating its well-repetitive and well-tuned nature. Asimov chain does not leave and enter more often except at factor 0.42, which shows its bad tuning. (**Reference: Initial state**)

In the case of the middle state as the reference (Figure 5.8), both chains follow the same pattern observed when the initial state is the reference. The adaptive fit oscillation chain leaves and enters the regeneration more often. In contrast, the Asimov chain rarely does that, indicating the well-tuned nature of the oscillation chain and the poorly tuned nature of the cross-section chain in the middle state as a reference.

The adaptive fit oscillation chain shows more entering and leaving pairs compared to the Asimov chain, which has a negligibly small number of entering and leaving pairs in both the initial (Figure 5.9) and middle states (Figure 5.10), as references. This indicates

the well-tuned or converged nature of the oscillation chain and the non-converged nature of the Asimov cross-section chain.

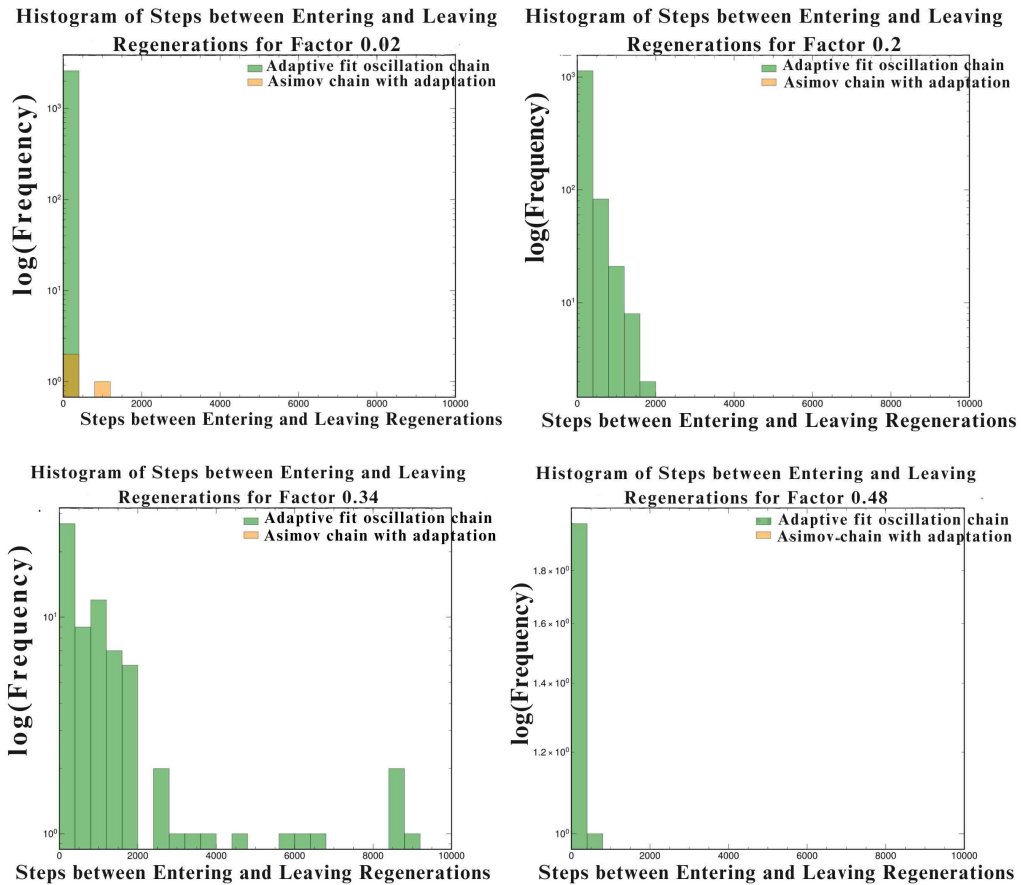


Figure 5.8: The steps between entering and leaving regeneration states dominate in the adaptive oscillation chain, indicating its well-repetitive and well-tuned nature. Asimov chain does not leave and enter more often, which shows its bad tuning. (**Reference: Middle state**)

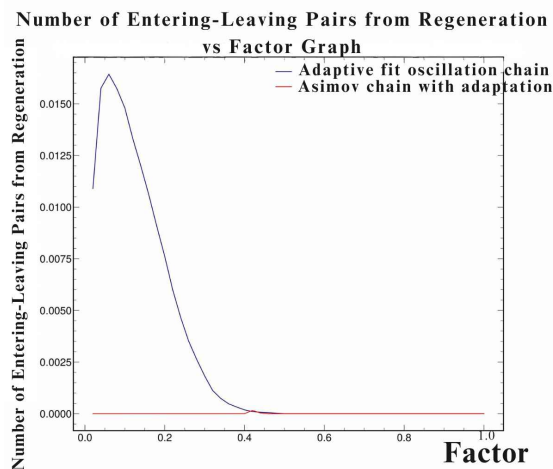


Figure 5.9: Adaptive oscillation chain has a significantly large number of entering and leaving regeneration pairs (**Reference: Initial state**)

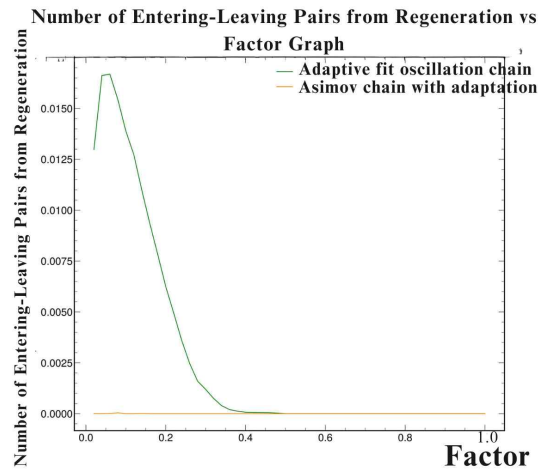


Figure 5.10: Adaptive oscillation chain has a significantly large number of entering and leaving regeneration pairs (**Reference: Middle state**)

### 5.3 Comparison of chains with and without adaptive step size tuning

This section compares adaptive and non-adaptive chains with many cross-section parameters, such as Asimov chains with and without adaptation, adaptive prior-only chain and non-adaptive chain, Asimov with adaptation and non-adaptive chain, and T2K near detector adaptive chain and non-adaptive chain. The difficulty of achieving convergence in Markov chains with many parameters makes the comparison studies using the regeneration diagnostic methods relevant.

#### 5.3.1 Asimov chain with adaptation vs. Asimov chain without adaptation

From the trace and autocorrelation plots of both of these long cross-section chains, it is evident that the Asimov chain with adaptation (Figure 5.11) does not explore parameter space by getting stuck in a state for a very long time and shows a high correlation between successive elements, which explains its poor nature. On the other hand, the Asimov chain without adaptation (Figure 5.12) explores the parameter space more often. It shows less correlation, making it a better chain than the adaptive cross-section chain.

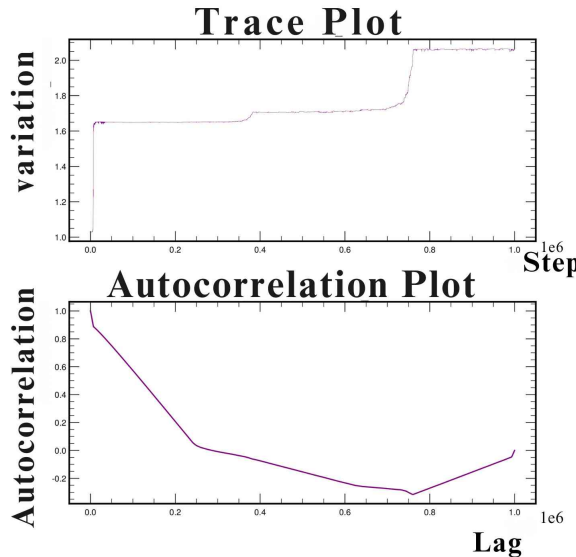


Figure 5.11: Trace and autocorrelation plots of Asimov chain with adaptation

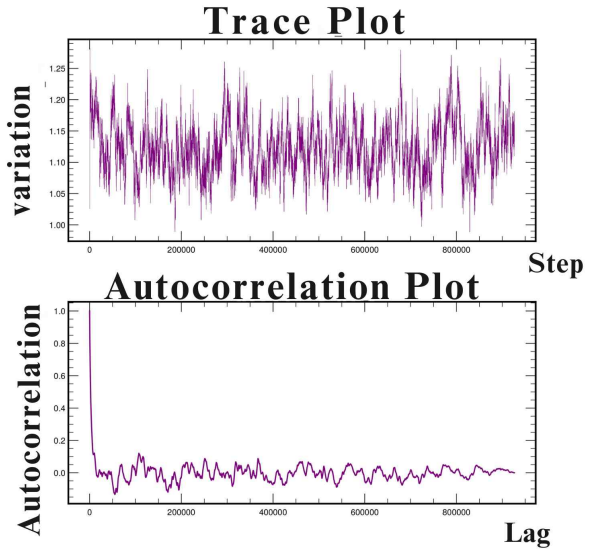


Figure 5.12: Trace and autocorrelation plots of Asimov chain without adaptation

In the case of the initial state (Figure 5.13) as a reference, the sudden spike in the number of regeneration states at factor 0.4 in the adaptive chain indicates that this chain

is not repeating enough. In contrast, the lack of a sudden spike in the non-adaptive chain suggests that this chain is repeating more often than the adaptive chain. In the case of the middle state (Figure 5.14) as a reference, the Asimov chain with adaptation shows a more significant number of regeneration states due to the flat nature of the trace plot than the non-adaptive chain. However, the wiggling behavior of the number of regenerations vs. factor plot of the adaptive chain picture this chain's non-repetitive and poorly tuned nature. At the same time, the non-adaptive cross-section chain shows a much smoother regeneration curve, demonstrating its good nature.

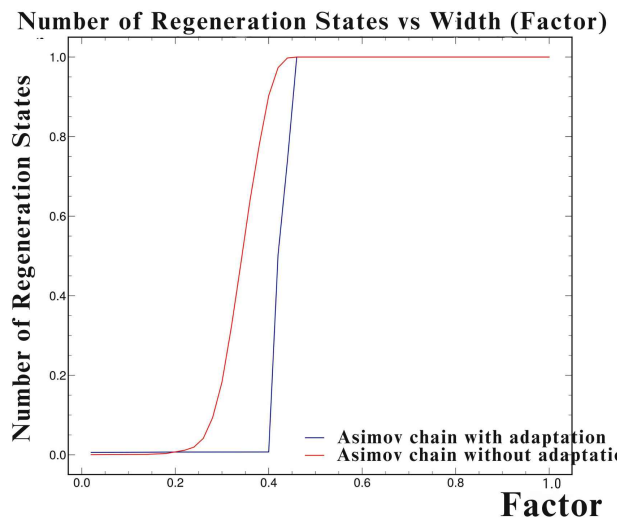


Figure 5.13: The comparison of variation in the number of regeneration states with the factor of Asimov chain with and without adaptation when the **initial state as reference**

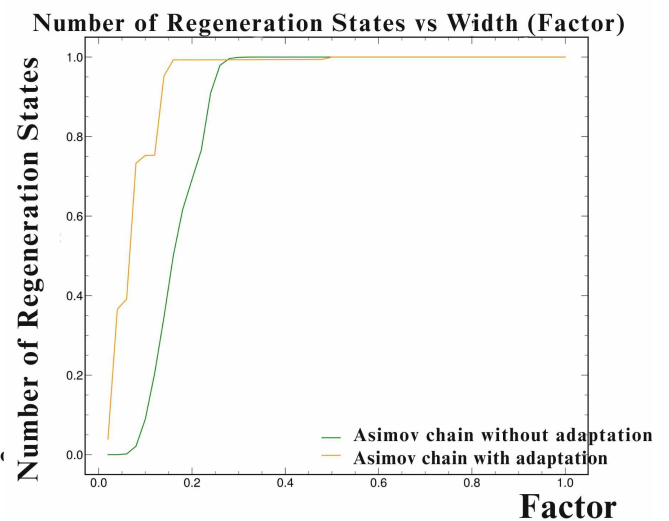


Figure 5.14: The comparison of variation in the number of regeneration states with the factor of Asimov chain with and without adaptation when the **middle state as reference**

The frequency plots of the steps between regeneration states and the steps between entering and leaving regenerations explicitly illustrate that the Asimov chain without adaptation shows more prominence over the adaptive cross-section chain in both of the initial and middle states as references, which indicates the well-tuned nature of the non-adaptive chain, shown in Figures 5.15, 5.16, 5.17, and 5.18.

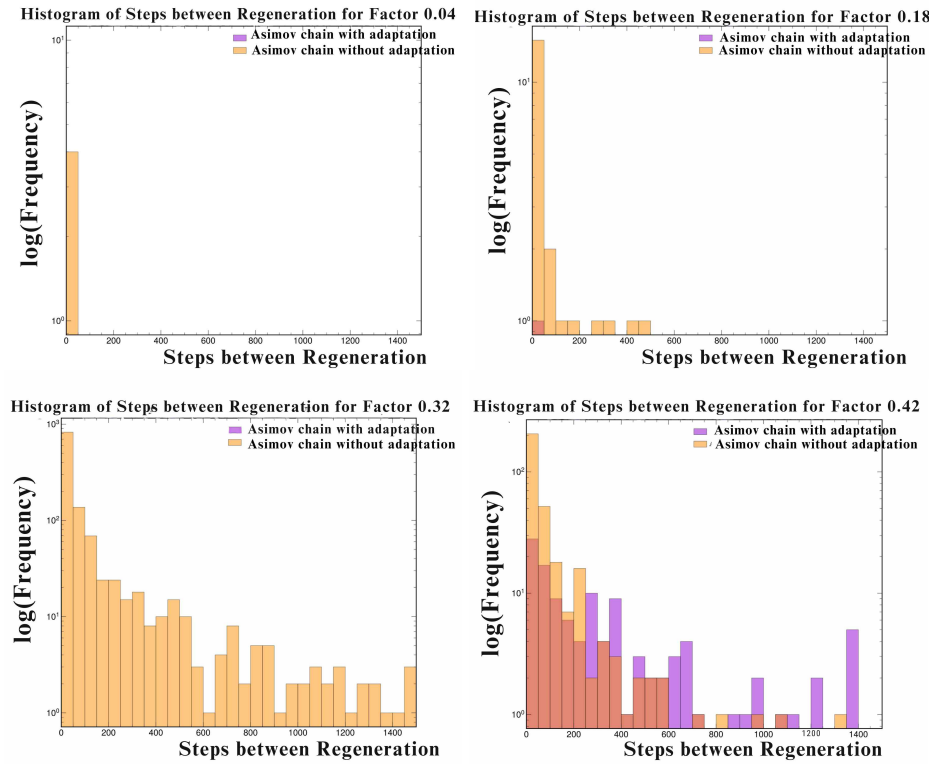


Figure 5.15: Asimov chain without adaptation has a significantly large number of steps between regenerations, indicating the better-tuned nature of this chain (**Reference: Initial state**)

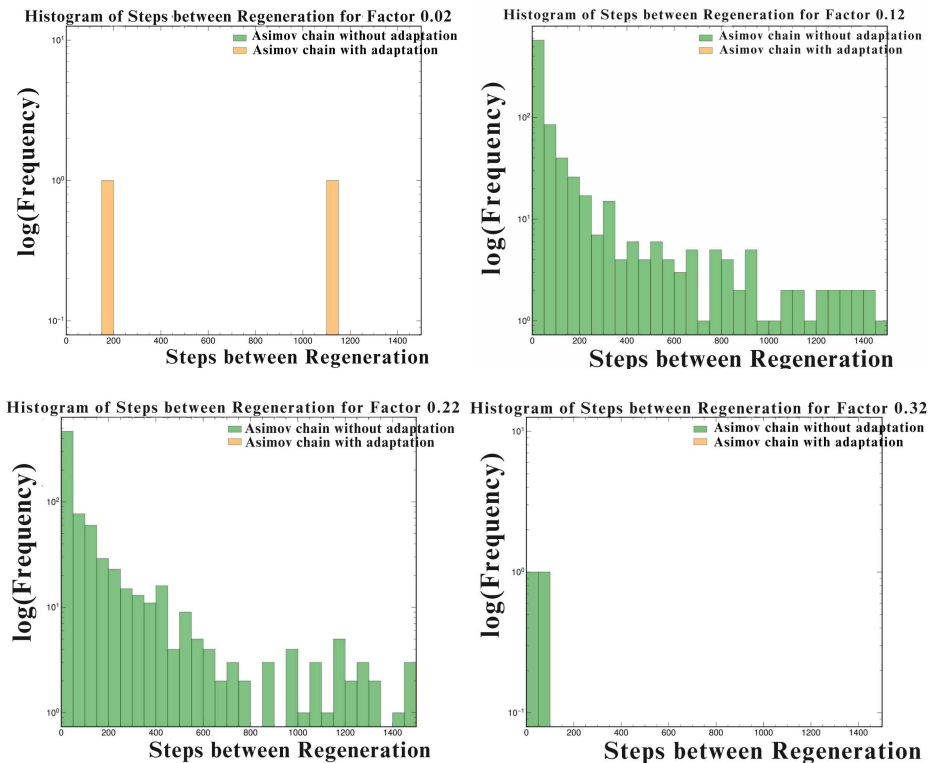


Figure 5.16: Asimov chain without adaptation has a significantly large number of steps between regenerations, indicating the better-tuned nature of this chain(**Reference: Middle state**)

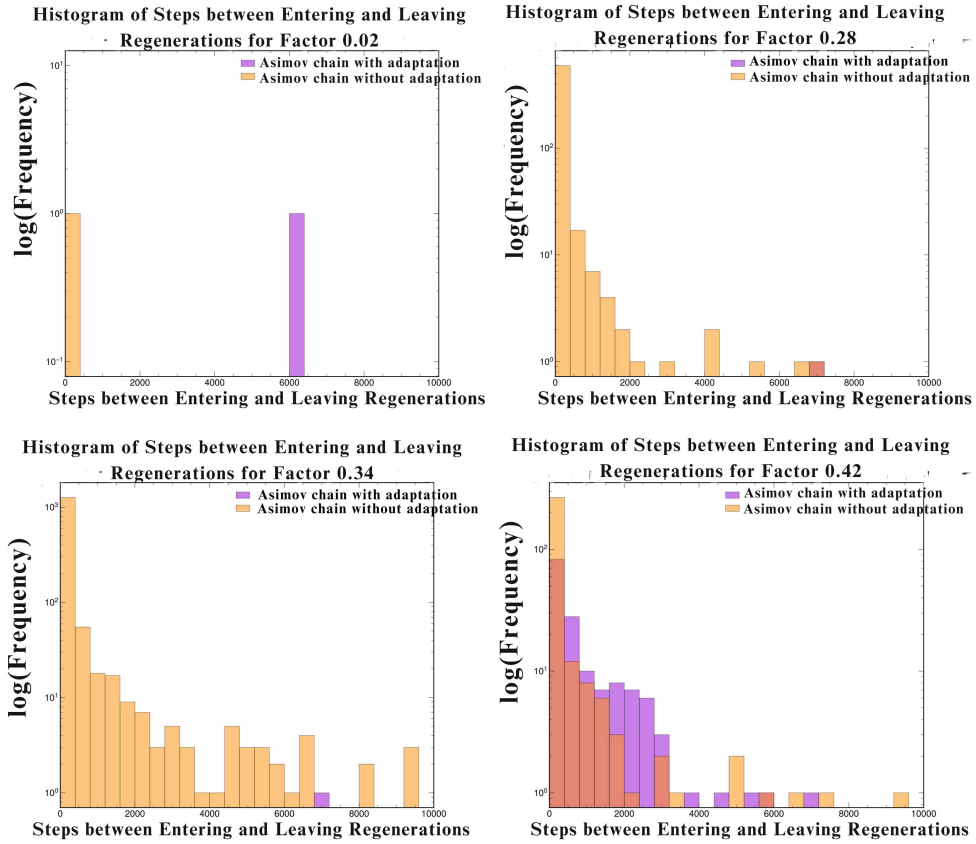


Figure 5.17: Asimov chain without adaptation has a significantly large number of steps between entering and leaving regenerations, indicating the better-tuned nature of this chain (**Reference: Initial state**)

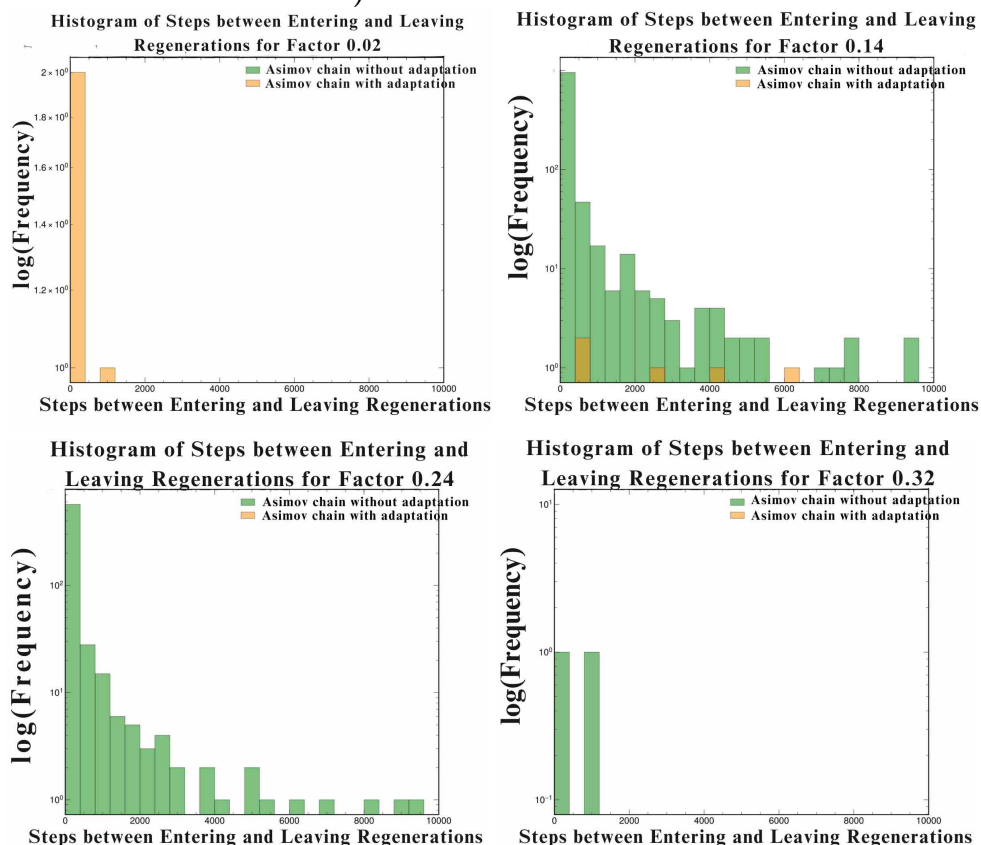


Figure 5.18: Asimov chain without adaptation has a significantly large number of steps between entering and leaving regenerations, indicating the better-tuned nature of this chain (**Reference: Middle state**)

The number of entering and leaving pairs dominates in the non-adaptive cross-section chain in both the initial (Figure 5.19) and middle (Figure 5.20) states as references compared to the adaptive chain, explaining the better nature of the non-adaptive chain over the adaptive chain.

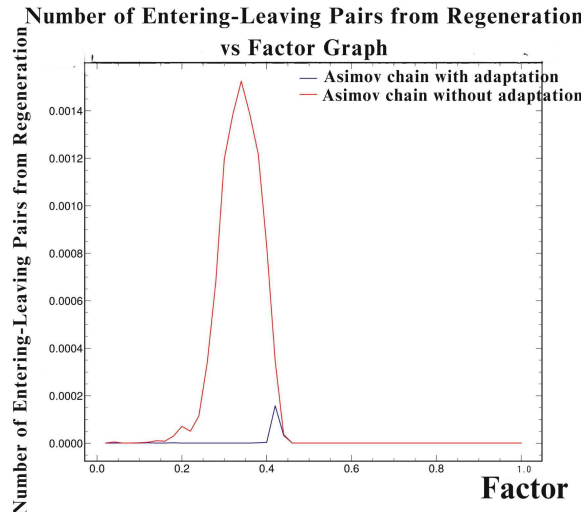


Figure 5.19: Asimov chain without adaptation has a significantly large number of entering and leaving regeneration pairs (Reference: Initial state)

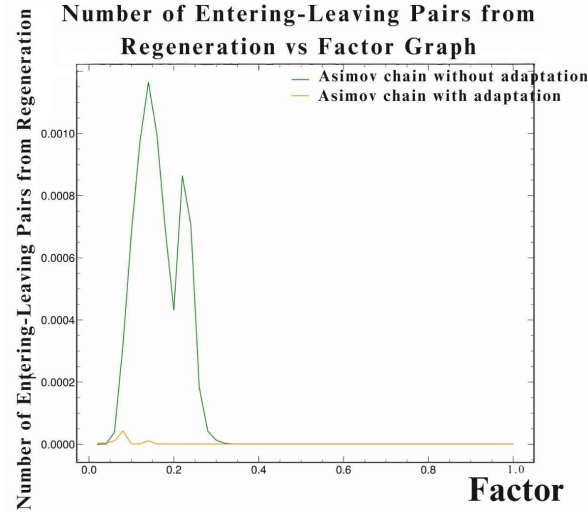


Figure 5.20: Asimov chain without adaptation has a significantly large number of entering and leaving regeneration pairs (Reference: Middle state)

### 5.3.2 Adaptive prior-only chain vs. Non-adaptive chain

The trace and autocorrelation plots of the adaptive prior-only (Figure 5.21) and non-adaptive cross-section chains demonstrate the prior-only chain's better-tuned nature and the non-adaptive chain's poorly-tuned nature. Because the prior-only chain explores the parameter space more frequently by entering and leaving states with significantly less correlation between successive elements. In contrast, the non-adaptive chain (Figure 5.22) behaves precisely the opposite.

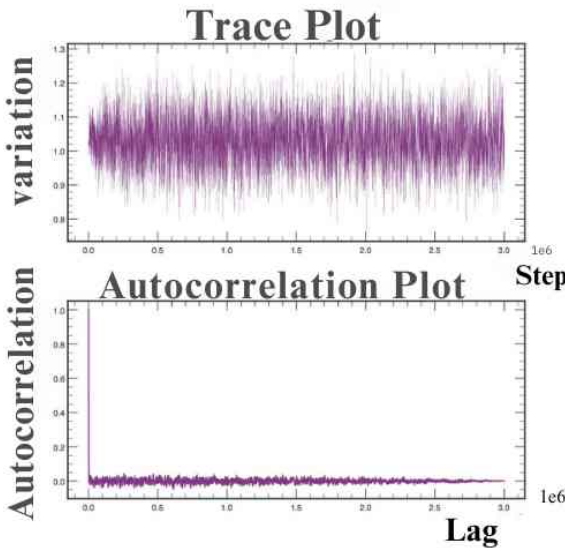


Figure 5.21: Trace and autocorrelation plots of Adaptive prior-only chain

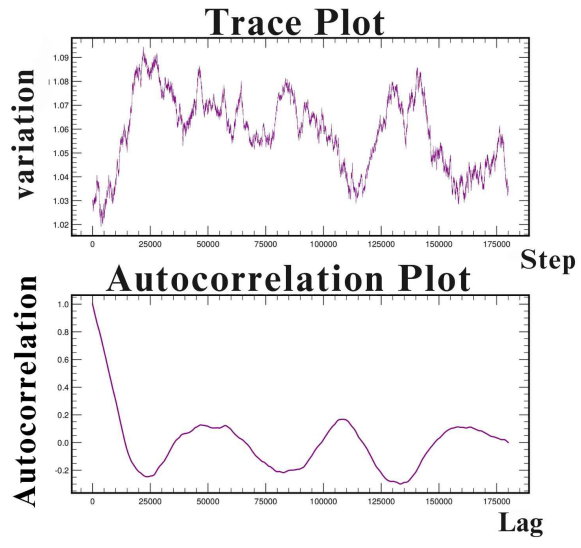


Figure 5.22: Trace and autocorrelation plots of Non-adaptive chain

In the case of the initial state as a reference (Figure 5.23), the gradual increase in the number of regeneration states without any wiggles in the prior-only chain agrees with its trace plot, substantiating its well-tuned behavior. On the other hand, non-smoothness in the non-adaptive chain portrays its poor tuning. However, when the middle state (Figure 5.24) is taken as a reference, the number of regeneration states vs. factor graph of both chains shows non-smoothness, which makes it hard to conclude.

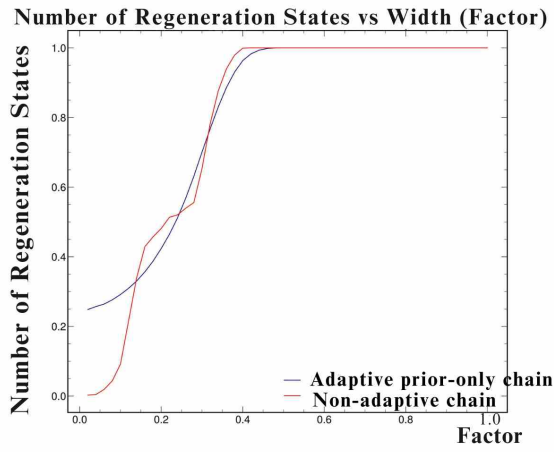


Figure 5.23: The comparison of variation in the number of regeneration states with the factor of adaptive prior-only chain and non-adaptive chain when the **initial state as reference**

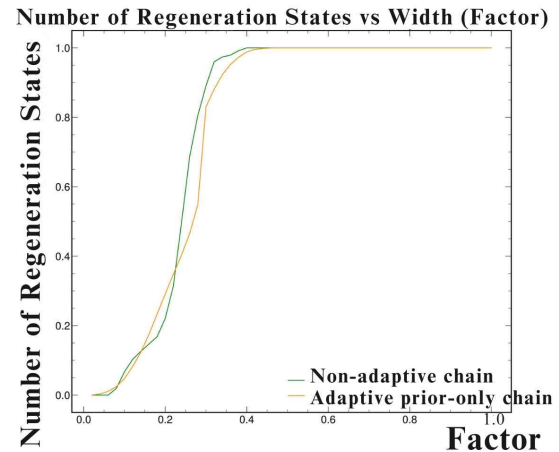


Figure 5.24: The comparison of variation in the number of regeneration states with the factor of adaptive prior-only chain and non-adaptive chain when the **middle state as reference**

The frequency of steps between regeneration and steps between entering and leaving regeneration in both the initial and middle states as references signify that the prior-only chain repeats more often, suggesting its well-tuned nature as expected, while the lower number of steps between regeneration and steps between entering and leaving regeneration in the non-adaptive chain explains its poorly tuned nature, shown in figures 5.25, 5.26, 5.27, and 5.28.

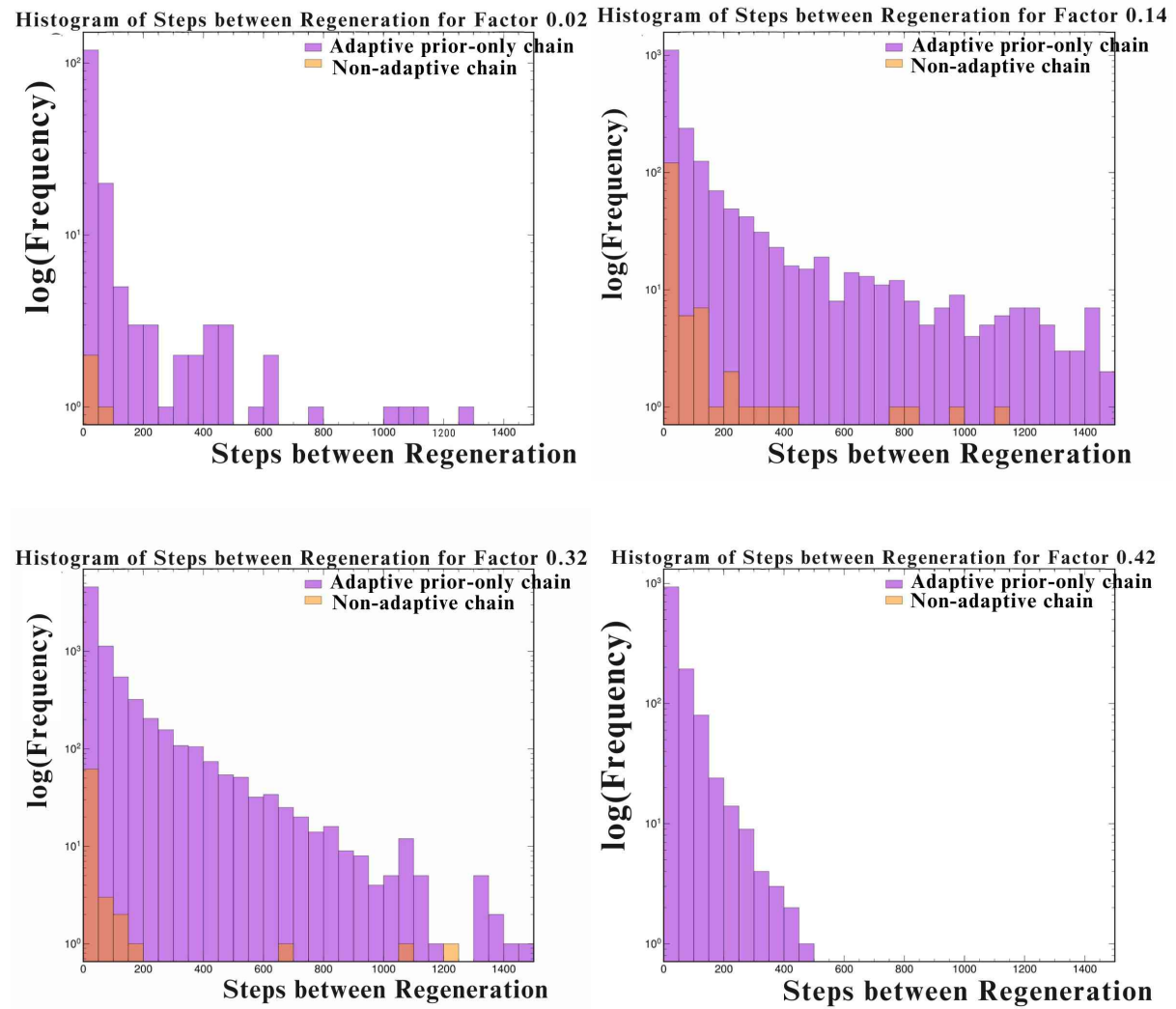


Figure 5.25: Adaptive prior-only chain has a significantly large number of steps between regenerations, indicating the better-tuned nature of this chain (**Reference: Initial state**)

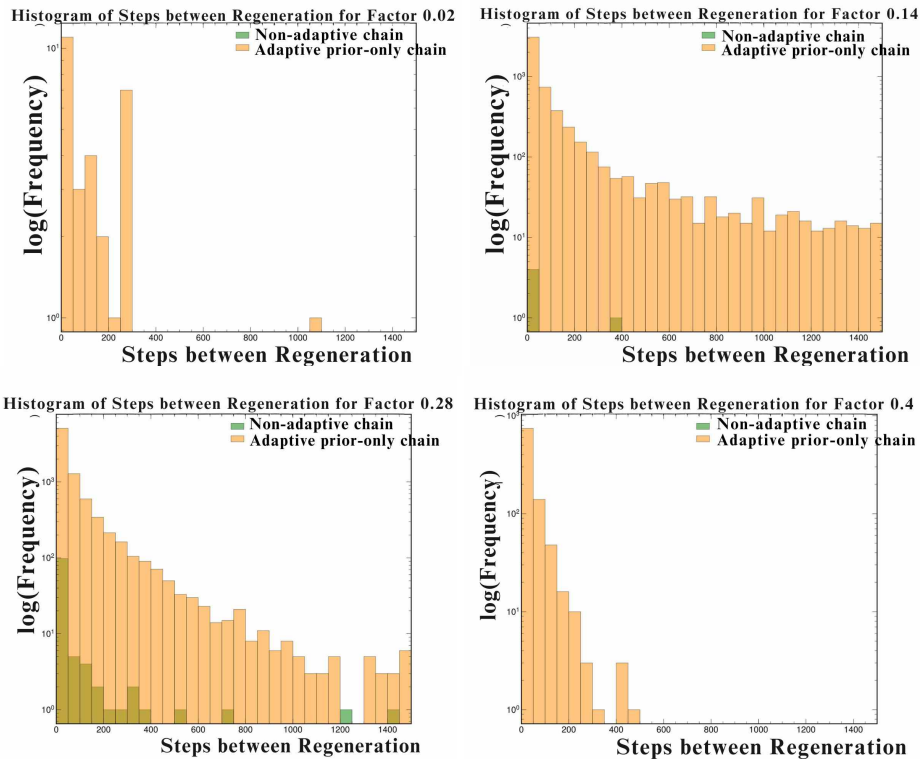


Figure 5.26: Adaptive prior-only chain has a significantly large number of steps between regenerations, indicating the better-tuned nature of this chain (**Reference: Middle state**)

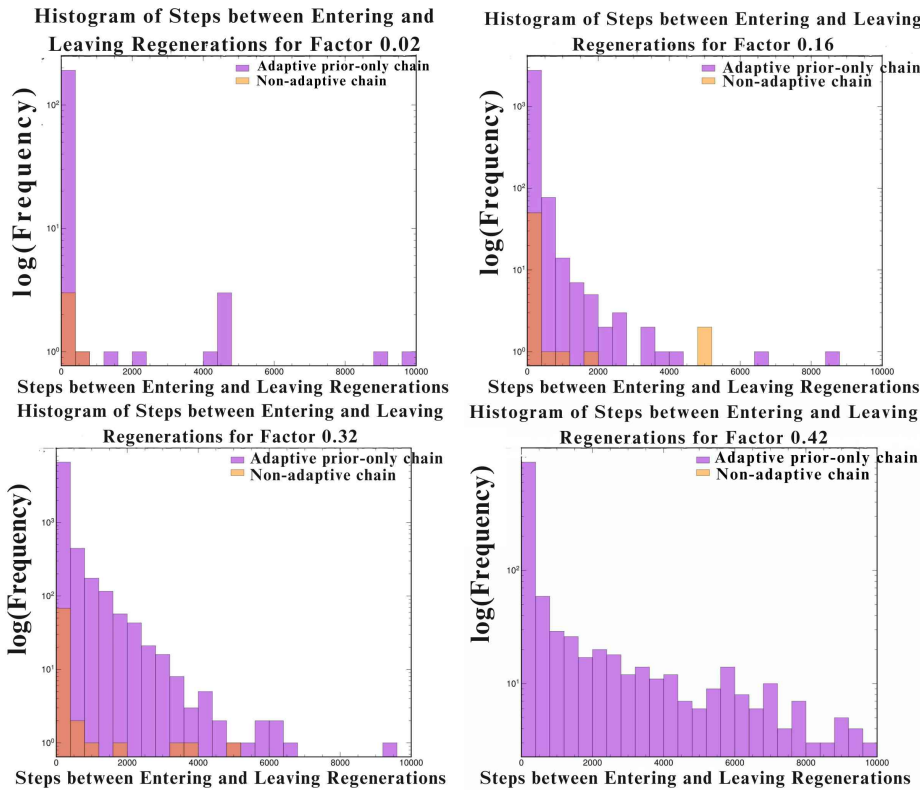


Figure 5.27: Adaptive prior-only chain has a significantly large number of steps between entering and leaving regenerations, indicating the better-tuned nature of this chain (**Reference: Initial state**)

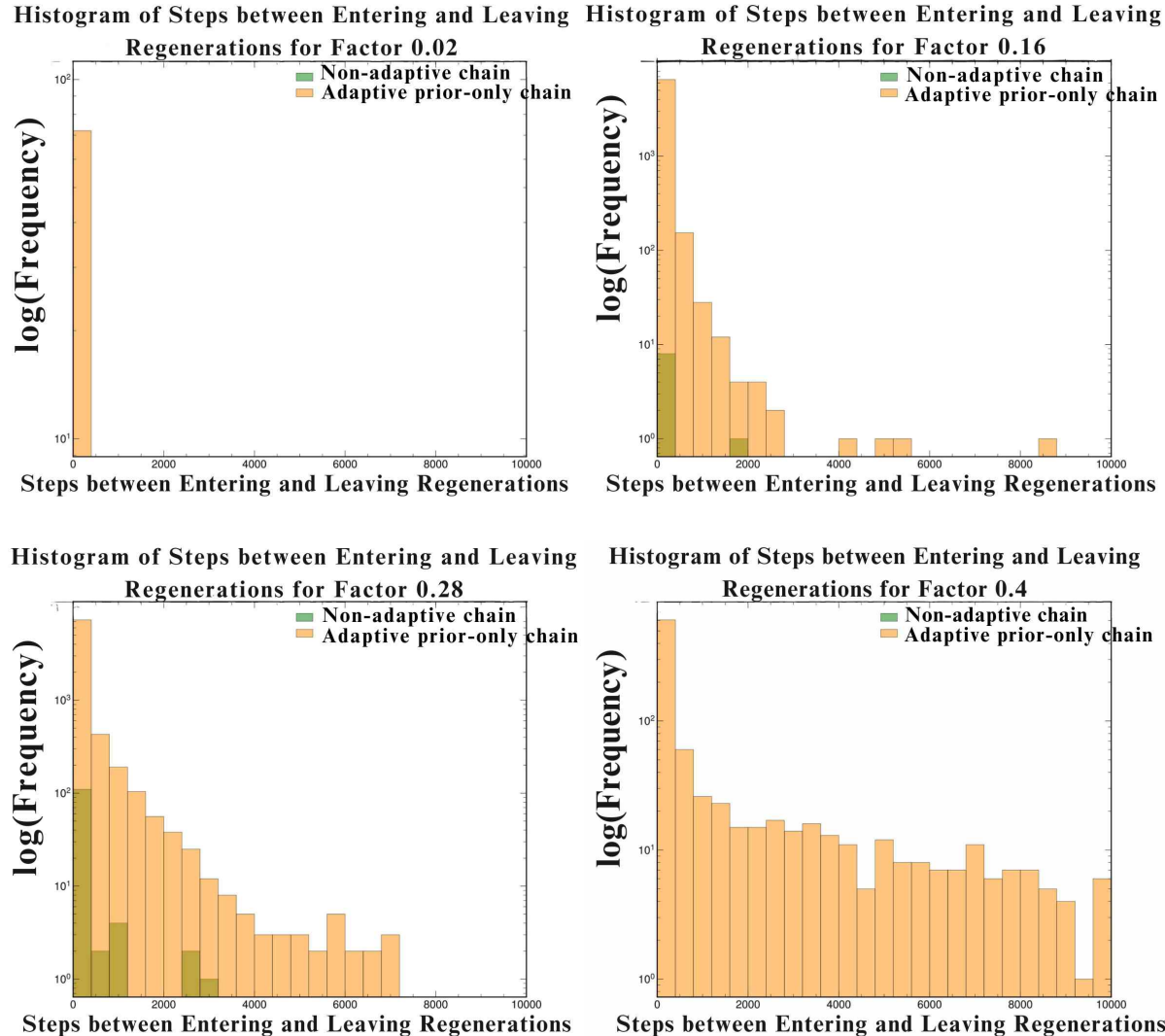


Figure 5.28: Adaptive prior-only chain has a significantly large number of steps between entering and leaving regenerations, indicating the better-tuned nature of this chain  
**(Reference: Middle state)**

Compared to the non-adaptive chain, the substantially higher number of entering and leaving pairs in the adaptive prior-only chain for both the initial (Figure 5.29) and middle (Figure 5.30) states as reference points demonstrate the superior tuning of the prior-only chain.

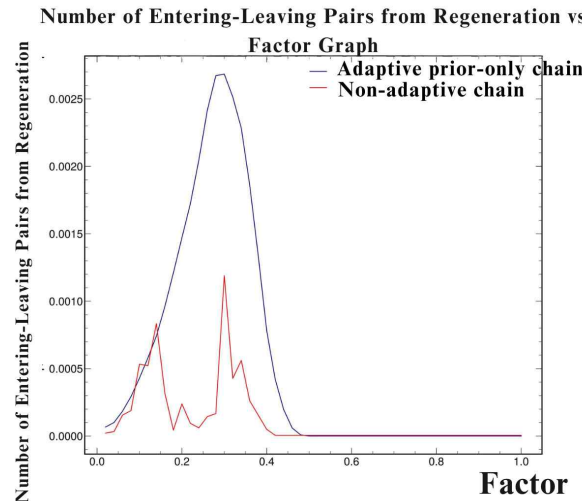


Figure 5.29: Adaptive prior-only chain has a significantly large number of entering and leaving regeneration pairs (**Reference: Initial state**)

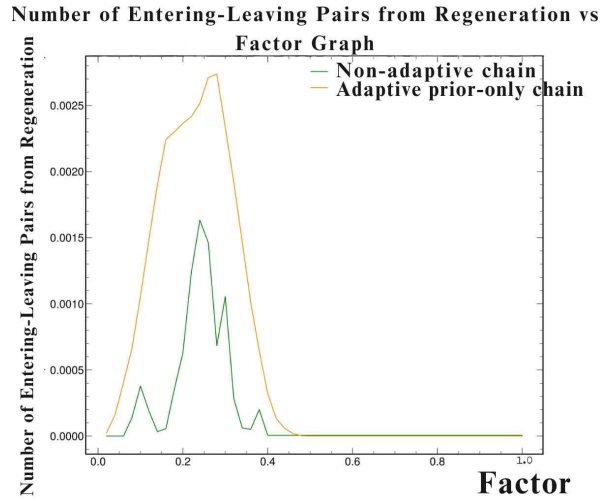


Figure 5.30: Adaptive prior-only chain has a significantly large number of entering and leaving regeneration pairs (**Reference: Middle state**)

### 5.3.3 Asimov chain with adaptation vs. Non-adaptive chain

The trace and autocorrelation plots of the cross-section parameter show that the Asimov chain gets stuck in a state for a long time (the middle part is flat) and does not explore the parameter space compared to the non-adaptive chain (Figure 5.31), indicating that the non-adaptive chain is better than the Asimov chain (Figure 5.32).

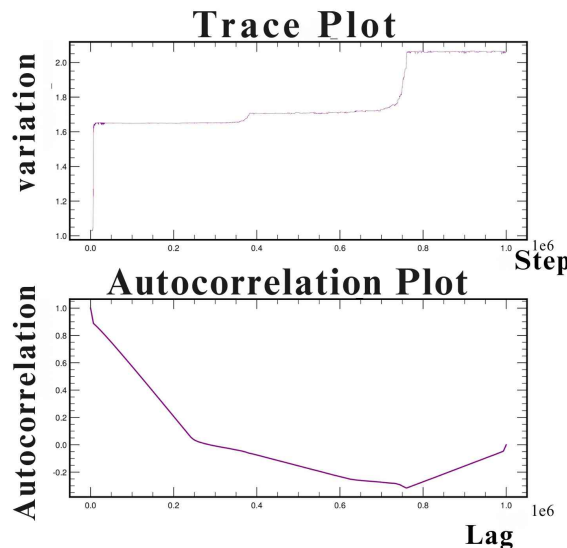


Figure 5.31: Trace and autocorrelation plots of Asimov chain with adaptation

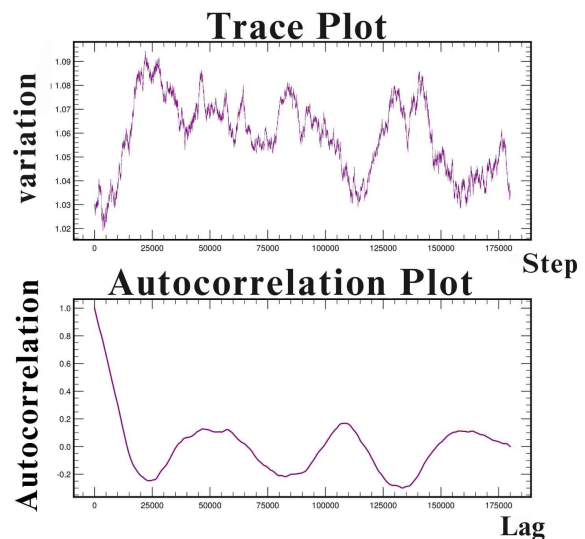


Figure 5.32: Trace and autocorrelation plots of Non-adaptive chain

When the initial state is the reference (Figure 5.33), the number of regeneration states increases in the non-adaptive chain much more gradually, indicating its better-tuned nature. At the same time, it is nearly constant till factor 0.42 in the Asimov chain, indicating its non-repetitive and poor-tuning nature. On the other hand, the number of regeneration states increases with factor in both the chains when the middle state is the reference (Figure 5.34); however, the non-smoothness in the Asimov chain represents its poor exploration of parameter space and tuning.

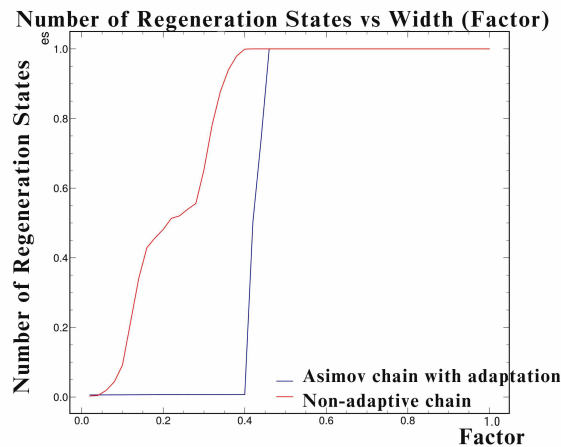


Figure 5.33: The comparison of variation in the number of regeneration states with the factor of Asimov chain with adaptation and non-adaptive chain when the **initial state as reference**

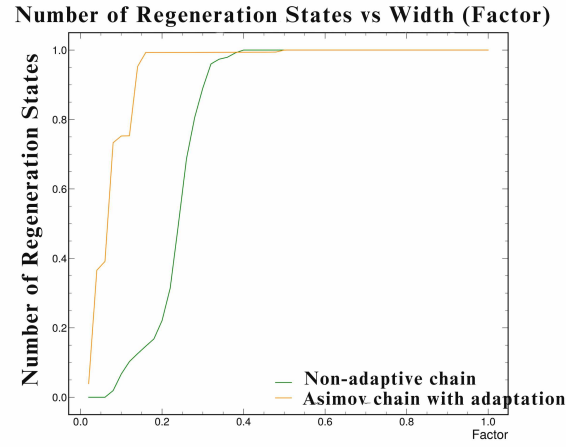


Figure 5.34: The comparison of variation in the number of regeneration states with the factor of Asimov chain with adaptation and non-adaptive chain when the **middle state as reference**

The steps between regeneration states dominate in the non-adaptive chain, with the initial (Figure 5.35) and middle (Figure 5.36) states as references, suggesting its better-tuned nature.

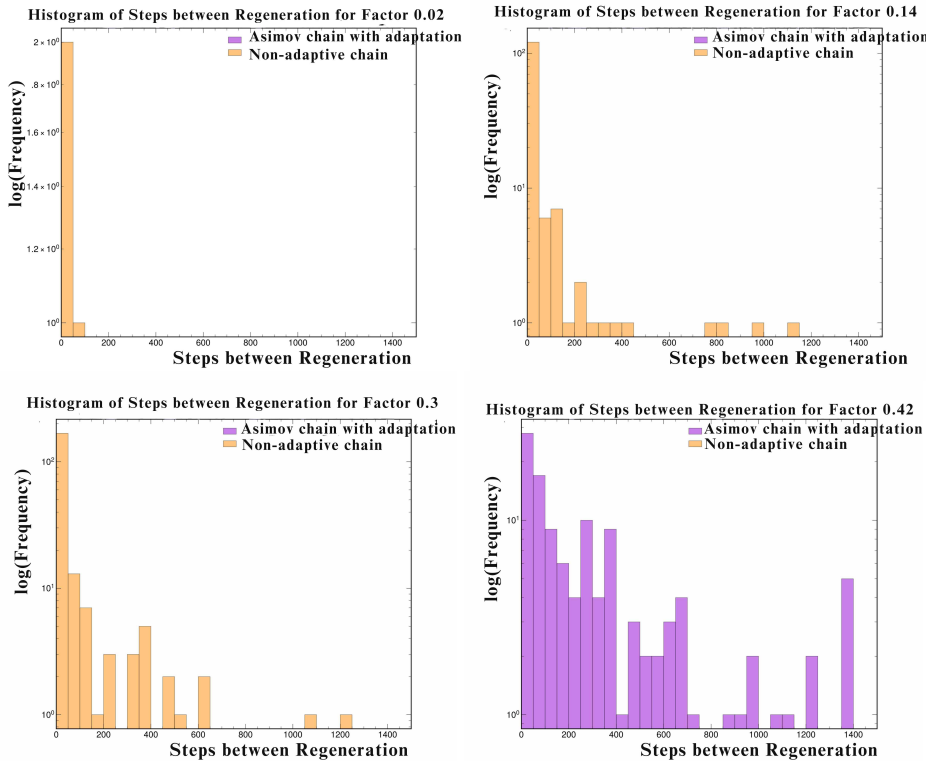


Figure 5.35: Non-adaptive chain has a significantly large number of steps between regenerations except at factor 0.42, indicating the better-tuned nature of this chain  
**(Reference: Initial state)**

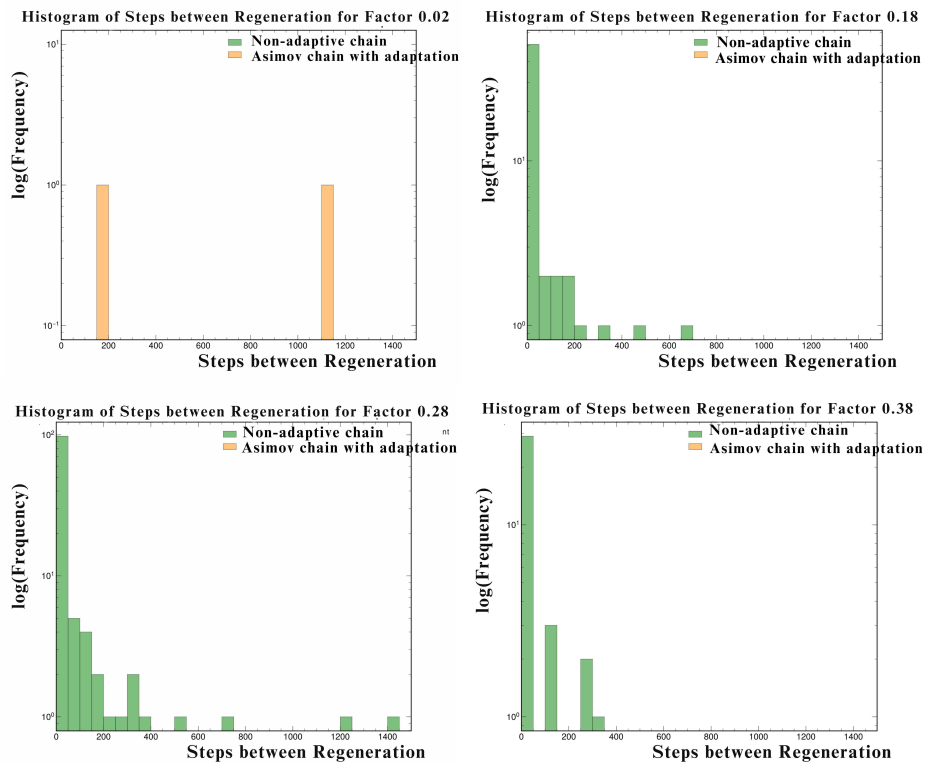


Figure 5.36: Non-adaptive chain has a significantly large number of steps between regenerations, indicating the better-tuned nature of this chain  
**(Reference: Middle state)**

The variation in the frequency of steps between entering and leaving regenerations, with the regeneration width as the initial state as a reference (Figure 5.37), portrays that the non-adaptive chain shows more steps between entering and leaving regenerations. This suggests that this chain repeats more often, stipulating its better-tuned nature. The scarcity of steps between entering and leaving regeneration states in the Asimov chain, except at factor 0.42, indicates its poorly tuned chain.

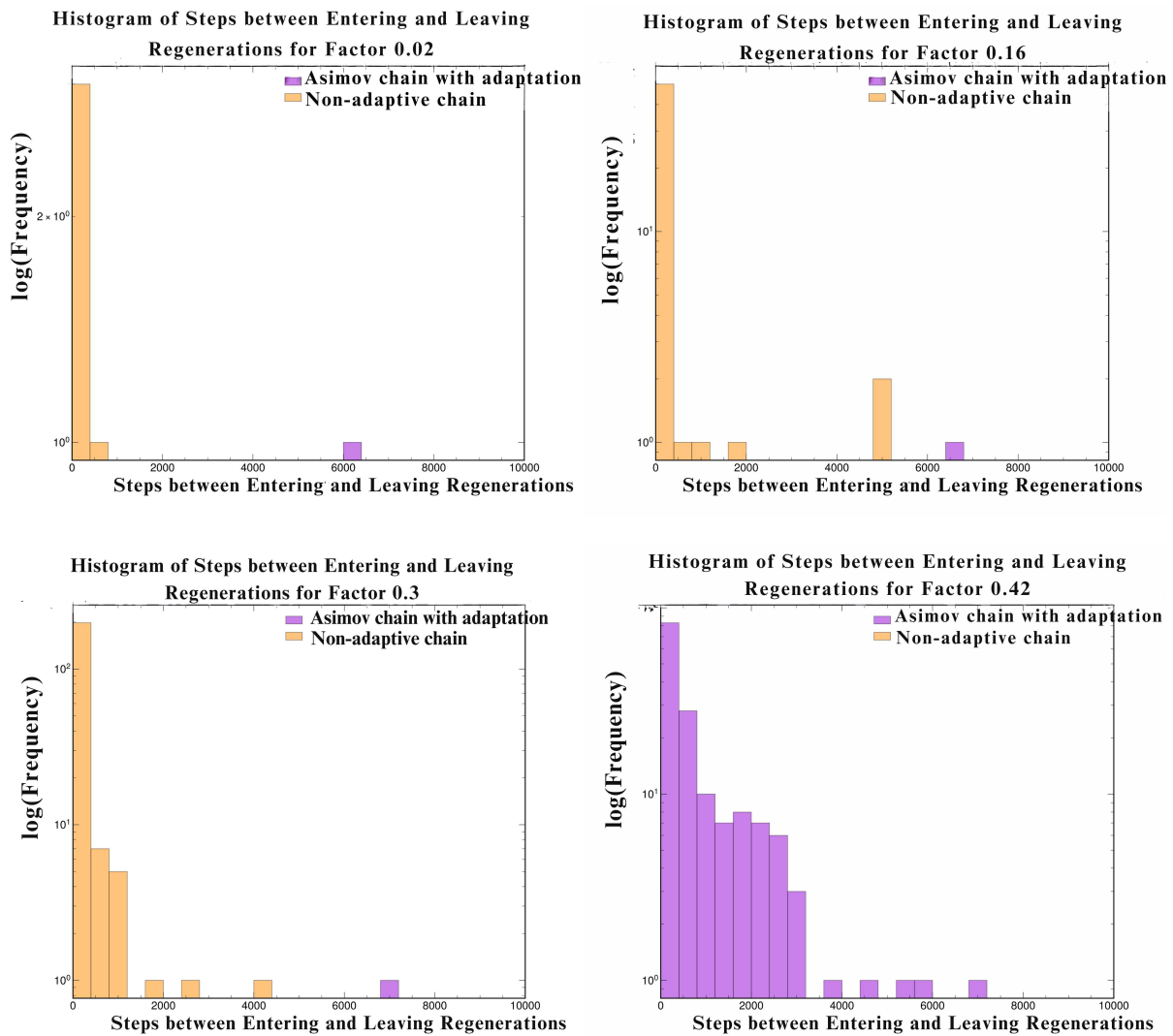


Figure 5.37: Non-adaptive chain shows more steps between entering and leaving regenerations except at factor 0.42, indicating the better-tuned nature of this chain  
**(Reference: Initial state)**

When the middle is the reference (Figure 5.38), the steps between entering and leaving regeneration states in the Asimov chain slightly dominate for the initial few factors; however, the non-adaptive chain has more steps between entering and leaving regeneration states in most of the factors, substantiating that the non-adaptive chain is better-tuned than the Asimov chain.

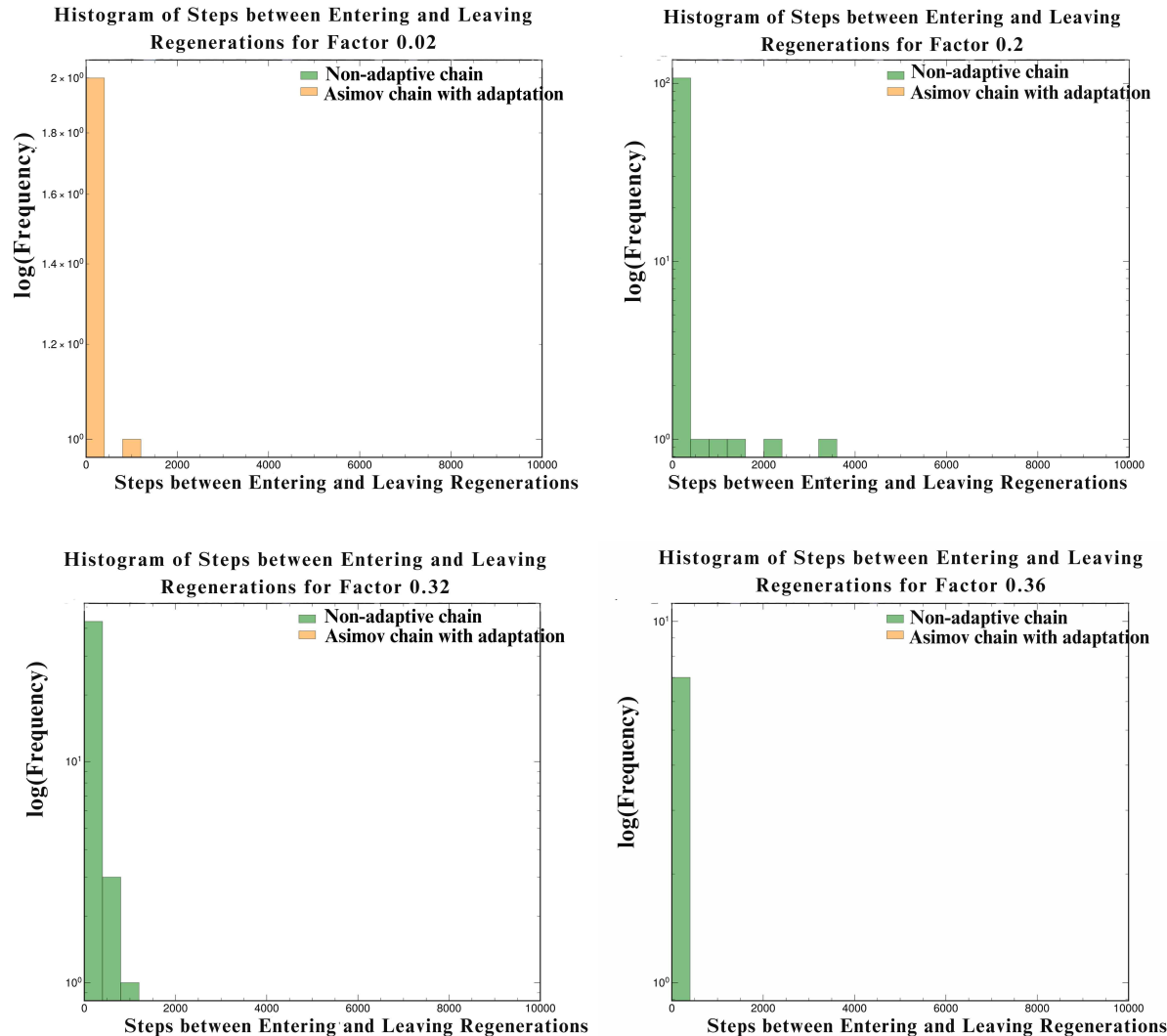


Figure 5.38: The steps between entering and leaving regeneration states dominate in the non-adaptive chain, indicating its well-repetitive and well-tuned nature, which is negligible in the Asimov chain, shows its bad tuning (**Reference: Middle state**)

The non-adaptive chain has a significantly larger number of entering and leaving pairs than the Asimov chain, which agrees well with the repetitive and well-tuned nature of the chain. In contrast, it is negligibly small in the Asimov chain, representing its poorly-tuned nature when initial (Figure 5.39) and middle (Figure 5.40) states are references.

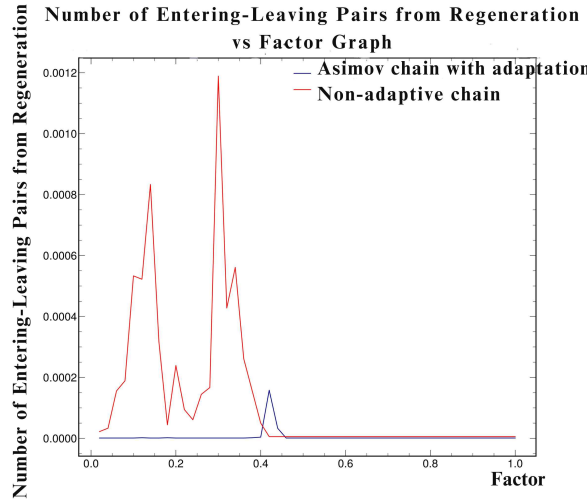


Figure 5.39: Non-adaptive chain has a significantly large number of entering and leaving regeneration pairs (**Reference: Initial state**)

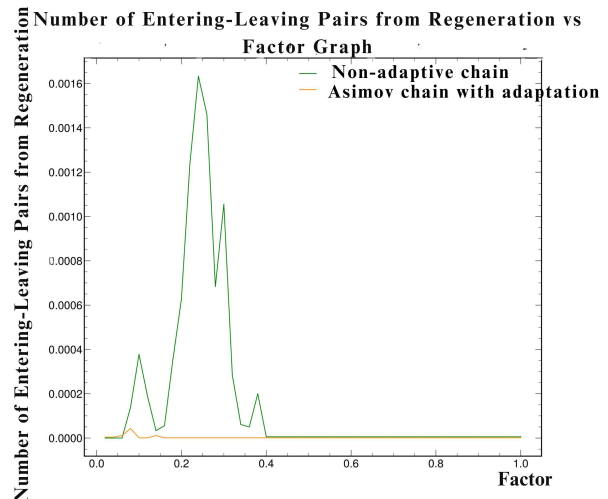


Figure 5.40: Non-adaptive chain has a significantly large number of entering and leaving regeneration pairs (**Reference: Middle state**)

### 5.3.4 T2K near detector adaptive chain vs. Non-adaptive chain

The trace and autocorrelation plots of the T2K near detector adaptive chain (Figure 5.41) specify that this chain repeats more often and is better tuned than the non-adaptive chain (Figure 5.42).

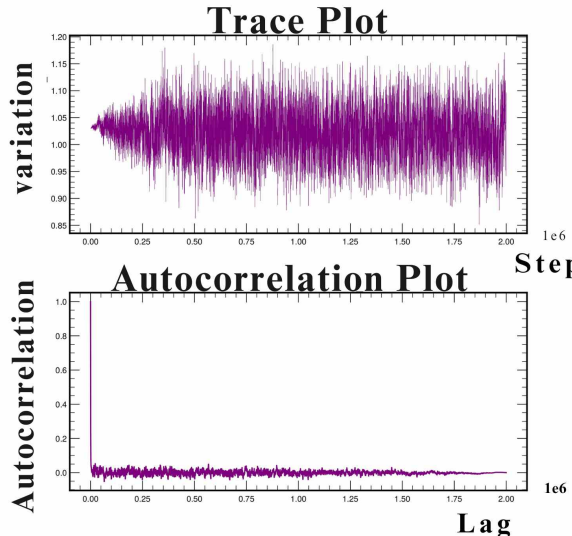


Figure 5.41: Trace and autocorrelation plots of T2K near detector adaptive chain

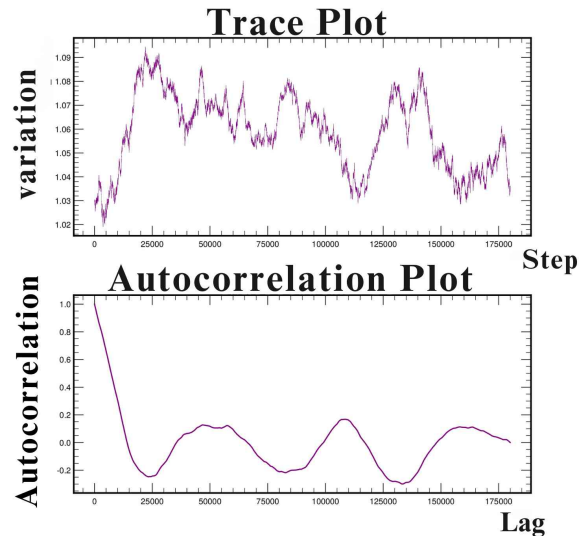


Figure 5.42: Trace and autocorrelation plots of Non-adaptive chain

T2K near detector adaptive chain shows a much smoother number of regeneration

states vs. factor curve when the initial state (Figure 5.43) is the reference than the non-adaptive chain, indicating that this adaptive chain is better-tuned than the non-adaptive chain. However, when the middle state (Figure 5.44) is the reference, both chains show a similar nature, which makes it difficult to compare their quality using this diagnostic tool.

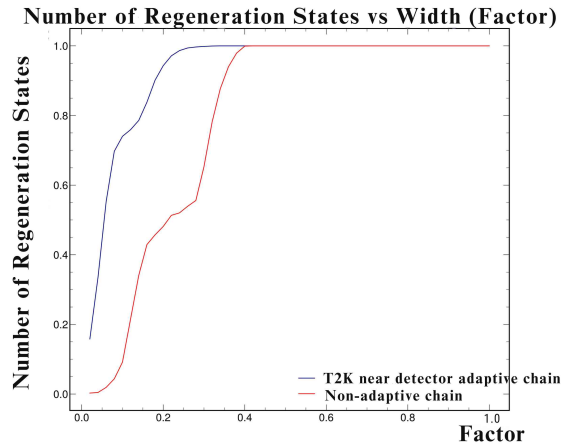


Figure 5.43: The comparison of variation in the number of regeneration states with the factor of T2K near detector adaptive chain and non-adaptive chain when the **initial state as reference**

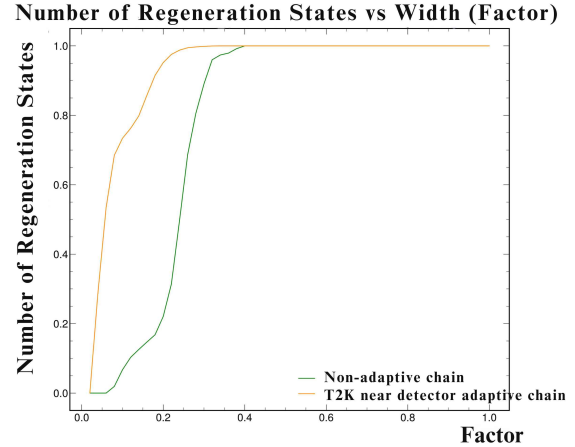


Figure 5.44: The comparison of variation in the number of regeneration states with the factor of T2K near detector adaptive chain and non-adaptive chain when the **middle state as reference**

The frequency of steps between regeneration states and steps between entering and leaving regeneration states histograms of all the factors for the initial and middle states as references indicate that the T2K near detector adaptive chain enters and leaves more often than the non-adaptive chain, suggesting its well-tuned nature, as shown in figures 5.45, 5.46, 5.47, and 5.48.

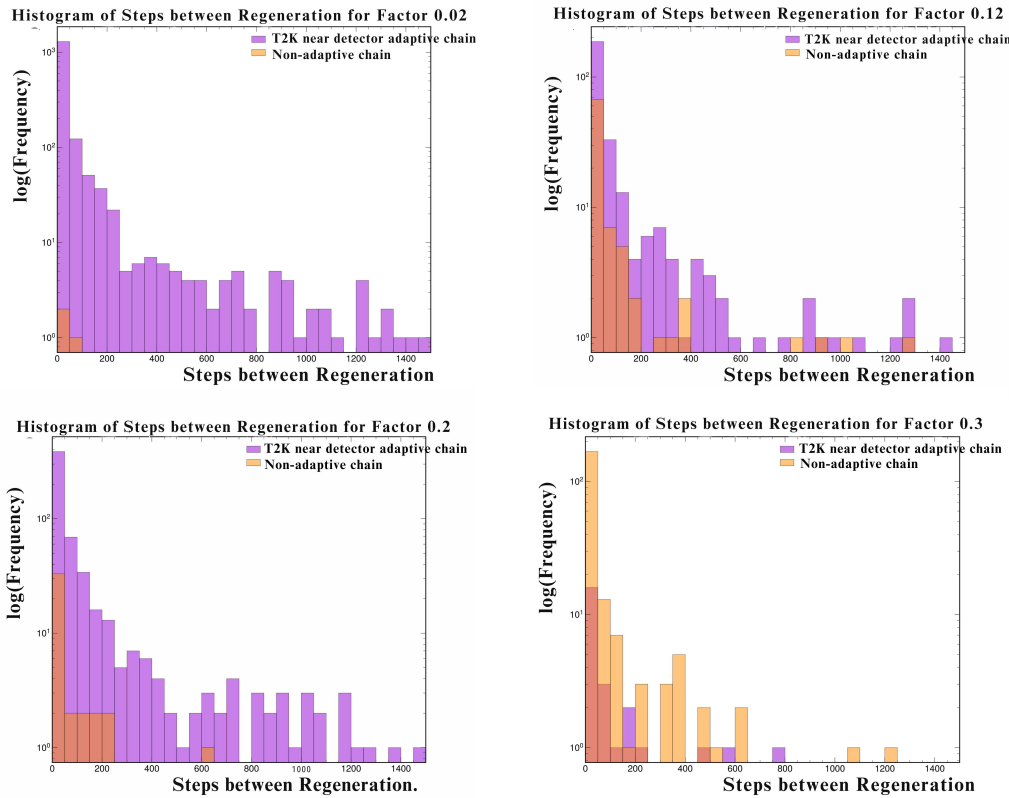


Figure 5.45: The steps between regeneration states dominate in the T2K near detector chain, indicating the chain's well-repetitive and well-tuned nature **Reference: Initial state**

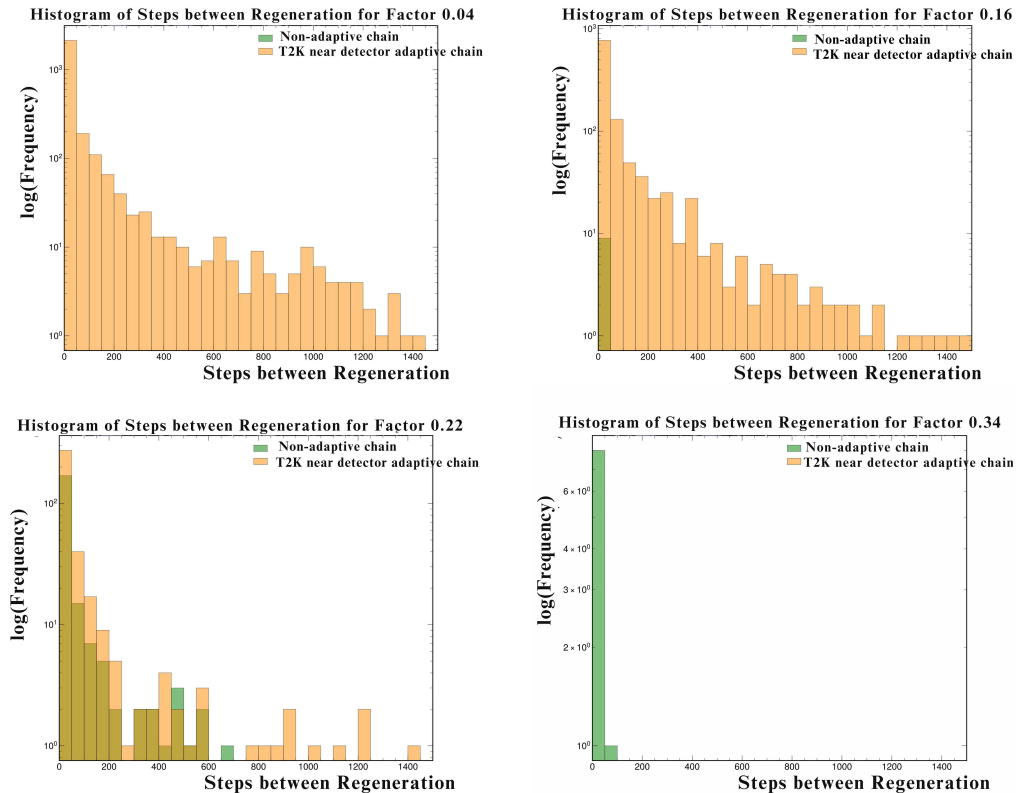


Figure 5.46: The steps between regeneration states dominate in the T2K near detector chain, indicating the chain's well-repetitive and well-tuned nature **Reference: Middle state**

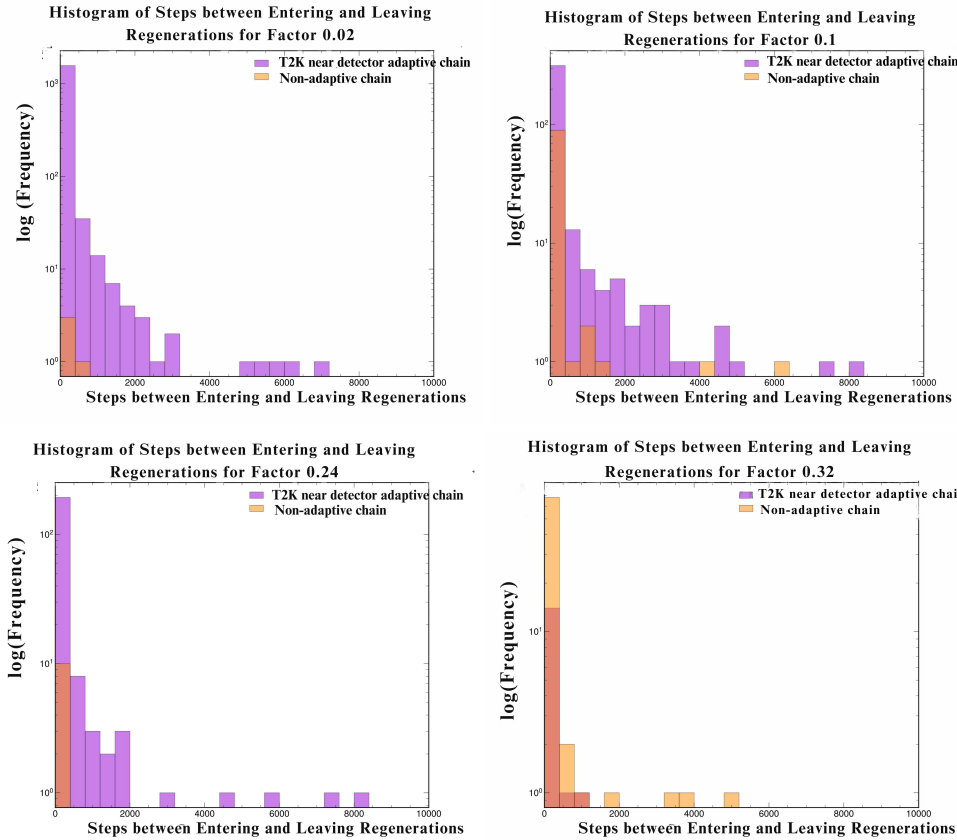


Figure 5.47: T2K near detector chain has a significantly large number of steps between entering and leaving regeneration states, indicating the better-tuned nature of this chain  
**(Reference: Initial state)**

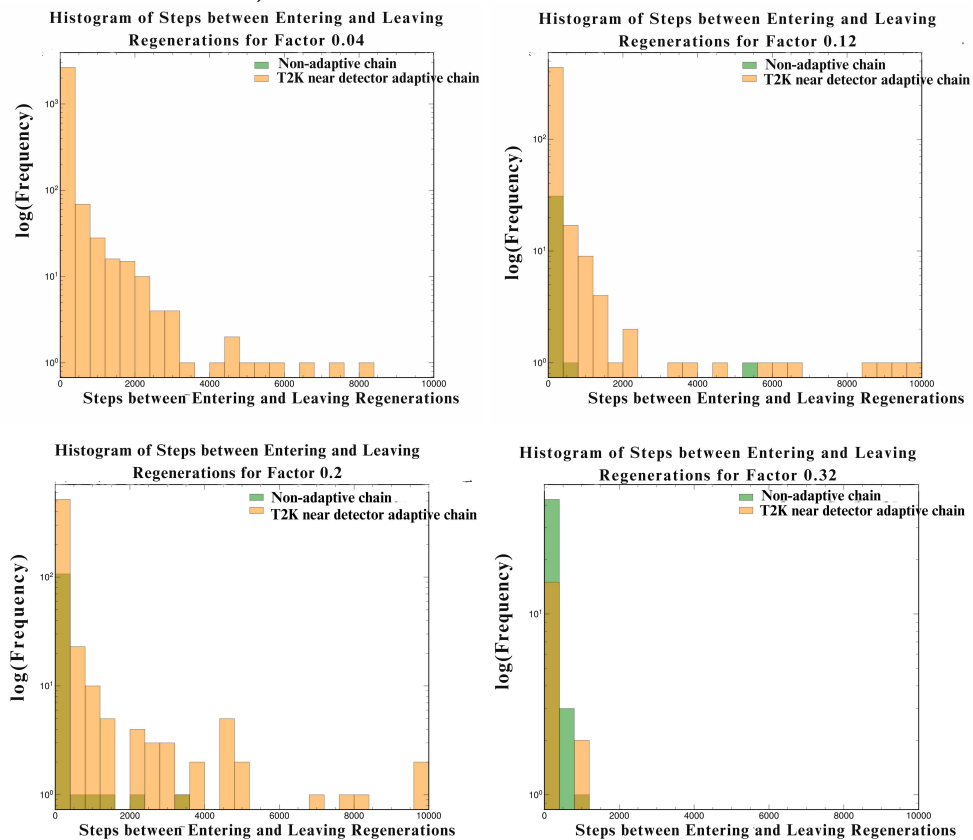


Figure 5.48: T2K near detector adaptive chain has a significantly large number of steps between entering and leaving regeneration states, indicating the better-tuned nature of this chain  
**(Reference: Middle state)** 63

A large number of entering and leaving pairs in both chains when initial (Figure 5.49) and middle (Figure 5.50) states are references makes this metric inconclusive enough to validate that the T2K near detector adaptive chain is better than the non-adaptive chain.

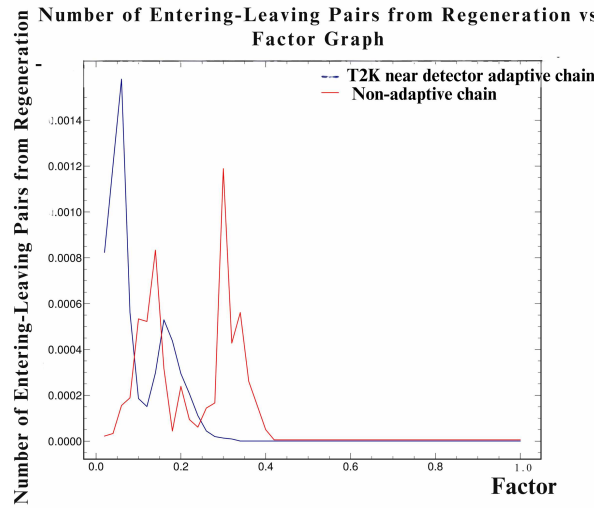


Figure 5.49: T2K near detector adaptive chain and Non-adaptive chain have a significantly large number of entering and leaving regeneration pairs (**Reference: Initial state**)

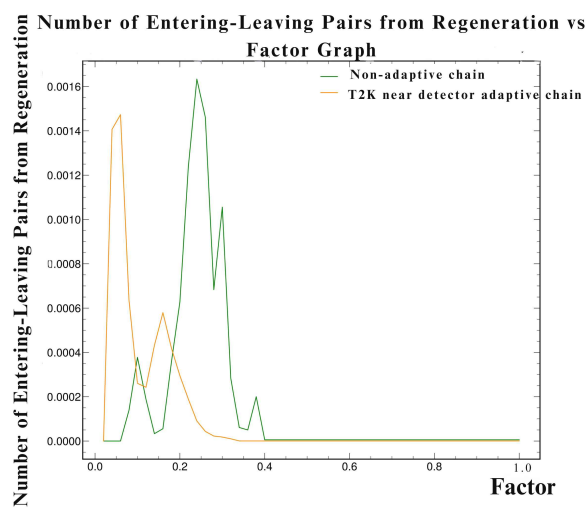


Figure 5.50: Non-adaptive chain has a slightly more number of entering and leaving regeneration pairs than the T2K near detector adaptive chain, which is misleading (**Reference: Middle state**)

## 5.4 Summary

The comparison of the Adaptive fit oscillation chain (six parameters) and the Asimov chain with adaptation (175 parameters) illustrated that the four regeneration diagnostic methods work well and are good assessment techniques to convey the well-tuned nature of the oscillation chain over the cross-section chain. However, the comparison of chains with many parameters is more interesting. It is observed that some of the regeneration diagnostic tools, such as the number of entering and leaving regeneration pairs vs. factor and the number of regeneration states vs. factor when the middle state is reference, are sometimes inefficient in assessing the quality of chains.

## 6. CONCLUSIONS AND OUTLOOK

This dissertation highlighted the importance of identifying regeneration states in a Markov chain and demonstrated how assessing the quality of chains can be enhanced using four diagnostic tools: ‘variation in the number of regeneration states with regeneration width (factor),’ ‘variation in the frequency of steps between regeneration states with regeneration width,’ ‘variation in the number of entering and leaving regeneration pairs with regeneration width,’ and ‘variation in the frequency of steps between entering and leaving regeneration states with regeneration width’. For the analysis, chains with both small and large numbers of parameters, as well as those with adaptive and non-adaptive step-size tuning, were compared using these four tools. Additionally, trace and autocorrelation plots were utilized to evaluate the effectiveness of these diagnostic methods.

Comparing chains with a few versus many parameters offers a straightforward method to evaluate the effectiveness of regeneration diagnostic tools. These tools prove to be effective in assessing chain quality, as evidenced by their ability to validate the well-tuned nature of the oscillation chain with just six parameters compared to the cross-section chain with 175 parameters.

Comparing cross-section chains with many parameters highlights the limitations of these diagnostic tools. For instance, in the comparison of the ’T2K near detector adaptive chain versus non-adaptive chain,’ the tools such as the variation in the number of regeneration states with regeneration width (using the middle state as a reference) and the variation in the number of entering and leaving pairs with regeneration width fail to definitively differentiate which chain performs better. Similarly, in comparing the ’adaptive prior-only chain versus non-adaptive chain’, the variation in the number of regeneration states with regeneration width (using the middle state as a reference) is also inconclusive. This analysis further reveals that ’frequency vs. steps between regenerations’ and ’frequency vs. steps between entering and leaving regenerations’ are more effective in evaluating the quality of chains considered here, aligning well with insights from trace and autocorrelation plots. Overall, using a combination of multiple regeneration tools along with trace and autocorrelation plots is crucial for a comprehensive analysis of Markov chain behavior.

## REFERENCES

- [1] Helen R. Quinn. "The Asymmetry between Matter and Antimatter". SLAC-PUB-9258, 2002. DOI: 10.1063/1.1564346.
- [2] A. Pich. "CP VIOLATION". CERN-TH.7114/93, 1993. <https://cds.cern.ch/record/256553/files/9312297.pdf>.
- [3] J. Chadwick. "Bakerian lecture.—The neutron". Royal Society of London, 1933. <https://doi.org/10.1098/rspa.1933.0152>.
- [4] W. Pauli. "Letter of the 4th December". 1930. <http://microboone-docdb.fnal.gov/cgi-bin/RetrieveFile?%20docid=953;filename=pauli%20letter1930.pdf>.
- [5] E. Fermi. "Versuch Einer Theorie der -Strahlen: I". Vol. vol. 88 (3-4) pp. 161–177. Zeitschrift für Physik, 1934. DOI: 10.1007/BF01351864.
- [6] F. Reines and C. L. Cowan. "Detection of the Free Neutrino". Vol. Phys. Rev. vol. 92 pp. 830–831. 1953. DOI: 10.1103/PhysRev.92.830.
- [7] C. L. Cowan et al. "Detection of the Free Neutrino: a Confirmation". Vol. Science vol. 124 (3212) pp. 103–104. 1956. DOI: 10.1126/science.124.3212.103.
- [8] Q. R. Ahmad et al. "Measurement of the Rate of  $\nu_e + d \rightarrow p + p + e^-$  Interactions Produced by  $^8B$  Solar Neutrinos at the Sudbury Neutrino Observatory.". Vol. Phys. Rev. Lett. 87, 071301. 2001. DOI: 10.1103/PhysRevLett.87.071301.
- [9] S. Fukuda et al. "Determination of Solar Neutrino Oscillation Parameters using 1496 days of Super-Kamiokande-I Data". Vol. Physics Letters B, 539(3):179 – 187. 2002. DOI: 10.1016/S0370-2693(02)02090-7.
- [10] F. Reines et al. "Detection of the Free Antineutrino". Vol. Phys. Rev. vol. 117 pp. 159–173. 1960. DOI: 10.1103/PhysRev.117.159.
- [11] F. Reines. "The Early Days of Experimental Neutrino Physics". Vol. Science vol. 203 (4375) pp. 11–16. 1979. DOI: 10.1126/science.203.4375.11.
- [12] R. Davis. "Attempt to Detect the Antineutrinos from a Nuclear Reactor by the  $Ci^{37}(\nu, e^-)A^{37}$  Reaction". Vol. Phys. Rev. vol. 97 pp. 766–769. 1955. DOI: 10.1103/PhysRev.97.766.

- [13] G. Danby et al. “*Observation of High-Energy Neutrino Reactions and the Existence of Two Kinds of Neutrino*”. Vol. Phys. Rev. Lett. vol. 9 pp. 36–44. 1962. DOI: [10.1103/PhysRevLett.9.36](https://doi.org/10.1103/PhysRevLett.9.36).
- [14] M. M. Block et al. “*Neutrino Interactions in the CERN Heavy Liquid Bubble Chamber*”. Vol. Physics Letters vol. 12 (3) pp. 281 – 285. 1964. DOI: [10.1016/0031-9163\(64\)91104-7](https://doi.org/10.1016/0031-9163(64)91104-7).
- [15] M. L. Perl et al. “*Evidence for Anomalous Lepton Production in  $e^+ - e^-$  Annihilation*”. Vol. Phys. Rev. Lett. vol. 35 pp. 1489–1492. 1975. DOI: [10.1103/PhysRevLett.35.1489](https://doi.org/10.1103/PhysRevLett.35.1489).
- [16] K. Kodama et al. “*Observation of Tau Neutrino Interactions*”. Vol. Physics Letters B vol. 504 (3) pp. 218 – 224. 2001. DOI: [10.1016/S0370-2693\(01\)00307-0](https://doi.org/10.1016/S0370-2693(01)00307-0).
- [17] The ALEPH Collaboration et al. “*Precision Electroweak Measurements on the Z Resonance*”. Vol. Physics Reports vol. 427 (5–6) pp. 257 – 454. 2006. DOI: [10.1016/j.physrep.2005.12.006](https://doi.org/10.1016/j.physrep.2005.12.006).
- [18] K. Abe et al. “*Observation of Electron Neutrino Appearance in a Muon Neutrino Beam*”. Vol. Phys. Rev. Lett., 112:061802. 2014. DOI: <https://doi.org/10.1103/PhysRevLett.112.061802>.
- [19] P. Adamson et al. “*First Measurement of Electron Neutrino Appearance in NOvA*”. Vol. Phys. Rev. Lett., 116:151806. 2016. DOI: <https://doi.org/10.1103/PhysRevLett.116.151806>.
- [20] D. S. Harmer R. Davis and K. C. Hoffman. “*Search for Neutrinos from the Sun*”. Vol. Phys. Rev. Lett. vol. 20 pp. 1205–1209. 1968. DOI: [10.1103/PhysRevLett.20.1205](https://doi.org/10.1103/PhysRevLett.20.1205).
- [21] B. Pontecorvo. “*Neutrino Experiments and the Problem of Conservation of Leptonic Charge*”. Vol. Journal of Experimental and Theoretical Physics vol. 26 pp. 984–988. 1968. DOI: <http://jetp.ac.ru/cgi-bin/e/index/e/26/5/p984?a=list>.
- [22] K. S. Hirata et al. “*Observation of  ${}^8B$  Solar Neutrinos in the Kamiokande-II Detector*”. Vol. Phys. Rev. Lett. vol. 63 pp. 16–19. 1989. DOI: [10.1103/PhysRevLett.63.16](https://doi.org/10.1103/PhysRevLett.63.16).

- [23] M. Cribier et al. “*Results of the Whole GALLEX Experiment*”. Vol. Nuclear Physics B - Proceedings Supplements vol. 70 (1–3) pp. 284 – 291. 1999. doi: [10.1016/S0920-5632\(98\)00438-1](https://doi.org/10.1016/S0920-5632(98)00438-1).
- [24] J. N. Abdurashitov et al. “*Solar Neutrino Flux Measurements by the Soviet-American Gallium Experiment (SAGE) for Half the 22-Year Solar Cycle*”. Vol. Journal of Experimental and Theoretical Physics vol. 95 (2) pp. 181–193. 2002. doi: [10.1134/1.1506424](https://doi.org/10.1134/1.1506424).
- [25] Q. R. Ahmad et al. “*Direct Evidence for Neutrino Flavor Transformation from Neutral-Current Interactions in the Sudbury Neutrino Observatory*”. Vol. Phys. Rev. Lett. vol. 89 p. 011301. 2002. doi: [10.1103/PhysRevLett.89.011301](https://doi.org/10.1103/PhysRevLett.89.011301).
- [26] T. Kajita et al. “*Establishing atmospheric neutrino oscillations with Super-Kamiokande*”. Vol. Nuclear Physics B. 2016. doi: <https://doi.org/10.1016/j.nuclphysb.2016.04.017>.
- [27] D. Casper et al. “*Measurement of Atmospheric Neutrino Composition with the IMB-3 Detector*”. Vol. Phys. Rev. Lett. vol. 66 pp. 2561–2564. 1991. doi: [10.1103/PhysRevLett.66.2561](https://doi.org/10.1103/PhysRevLett.66.2561).
- [28] Y. Fukuda et al. “*Atmospheric  $\nu_\mu/\nu_e$  Ratio in the Multi-GeV Energy Range*”. Vol. Physics Letters B vol. 335 (2) pp. 237 – 245. 1994. doi: [10.1016/0370-2693\(94\)91420-6](https://doi.org/10.1016/0370-2693(94)91420-6).
- [29] K. Eguchi et al. (KamLAND Collaboration). “*First Results from KamLAND: Evidence for Reactor Antineutrino Disappearance*”. Vol. Phys. Rev. Lett. vol. 90 p. 021802. 2003. doi: [doi:10.1103/PhysRevLett.90.021802](https://doi.org/10.1103/PhysRevLett.90.021802).
- [30] J. K. Ahn et al. “*Observation of Reactor Electron Antineutrinos Disappearance in the RENO Experiment*”. Vol. Phys. Rev. Lett. 108, 191802. 2012. doi: <https://doi.org/10.1103/PhysRevLett.108.191802>.
- [31] F. P. An et al. “*Observation of Electron-Antineutrino Disappearance at Daya Bay*”. Vol. Phys. Rev. Lett. 108, 171803. 2012. doi: <https://doi.org/10.1103/PhysRevLett.108.171803>.
- [32] M. Apollonio et al. “*Search for neutrino oscillations on a long base-line at the CHOOZ nuclear power station*”. Vol. Eur. Phys. J., 27. 2003. doi: [https://doi.org/10.48550/arXiv.hep-ex/0301017](https://arxiv.org/abs/hep-ex/0301017).

- [33] Y. Abe et al. “*Measurement of  $\theta_{13}$  in Double Chooz using neutron captures on hydrogen with novel background rejection techniques*”. Vol. Journal of High Energy Physics, 163. 2016. DOI: [https://doi.org/10.1007/JHEP01\(2016\)163](https://doi.org/10.1007/JHEP01(2016)163).
- [34] M. H. Ahn et al. (K2K Collaboration). “*Measurement of neutrino oscillation by the K2K experiment*”. Vol. Phys. Rev. D 74, 072003. 2006. DOI: <https://doi.org/10.1103/PhysRevD.74.072003>.
- [35] D. G. Michael et al. “*Observation of Muon Neutrino Disappearance with the MINOS Detectors in the NuMI Neutrino Beam*”. Vol. Phys. Rev. Lett. 97, 191801. 2006. DOI: <https://doi.org/10.1103/PhysRevLett.97.191801>.
- [36] R. Acquafredda et al. “*The OPERA experiment in the CERN to Gran Sasso neutrino beam*”. Vol. Journal of Instrumentation. 2009. DOI: [10.1088/1748-0221/4/04/P04018](https://doi.org/10.1088/1748-0221/4/04/P04018).
- [37] B. Kayser. “*Neutrino Physics*”. Vol. eConf vol. C040802 p. L004. 2004. DOI: <https://doi.org/10.48550/arXiv.hep-ph/0506165>.
- [38] A. Gando et al. (KamLAND Collaboration). “*Reactor On-Off Antineutrino Measurement With KamLAND*”. Vol. Phys. Rev. D vol. 88 p. 033001. 2013. DOI: [10.1103/PhysRevD.88.033001](https://doi.org/10.1103/PhysRevD.88.033001).
- [39] Charlie Naseby. “*Understanding the impact of an expanded neutral current pion production model on long-baseline oscillation analyses at T2K*”. Vol. PhD Thesis Imperial College, London. 2023. DOI: [10.25560/106385](https://doi.org/10.25560/106385).
- [40] S. Richardson W. R. Gilks and D. J. Spiegelhalter. “*Markov Chain Monte Carlo in Practice*”. Vol. (Chapman Hall/CRC Interdisciplinary Statistics). 1995. DOI: [ChapmanandHall/CRC](https://doi.org/10.1201/9780429119744).
- [41] Galin L. Jones and Qian Qin. “*Markov Chain Monte Carlo in Practice*”. Vol. Annu. Rev. Stat. Appl. 9:557-578. 2022. DOI: <https://doi.org/10.1146/annurev-statistics-040220-090158>.
- [42] Kirsty Elizabeth Duffy. “*Measurement of the neutrino oscillation parameters  $\sin^2 \theta_{23}$ ,  $\Delta m_{32}^2$ ,  $\sin^2 \theta_{13}$ , and  $\delta_{CP}$  in neutrino and antineutrino oscillation at T2K*”. Vol. PhD Thesis University of Oxford. 2016. DOI: [Thesis\\_KDuffy\\_libraryversion\\_20170223.pdf](https://doi.org/10.21437/PhD-Thesis-KDuffy-20170223).

- [43] Michael Dolce. “*Constraining neutrino oscillation and interaction parameters with the NOvA Near Detector and Far Detector data using Markov Chain Monte Carlo*”. Vol. PhD Thesis Tufts University. 2016.
- [44] J. Dunkley et al. “*Fast and Reliable Markov Chain Monte Carlo Technique for Cosmological Parameter Estimation*”. Vol. Monthly Notices of the Royal Astronomical Society vol. 356 (3) pp. 925–936. 2005. DOI: [10.1111/j.1365-2966.2004.08464.x](https://doi.org/10.1111/j.1365-2966.2004.08464.x).
- [45] Will Parker. “*Constraining Systematic Uncertainties at T2K using Near Detector Data*”. Vol. PhD Thesis Royal Holloway, University London. 2020.
- [46] Carl Vincent Clarence Wret. “*Minimising Systematic Uncertainties in the T2K Experiment Using Near-Detector and External Data*”. Vol. PhD Thesis Imperial College London. 2018. DOI: [10.25560/73862](https://doi.org/10.25560/73862).
- [47] Anthony E. Brockwell and Joseph B. Kadane. “*Identification of Regeneration Times in MCMC Simulation, with Application to Adaptive Schemes*”. Vol. Journal of Computational and Graphical Statistics, Vol. 14, No. 2, pp. 436-458. 2005. <https://www.jstor.org/stable/27594123>.
- [48] M. A. Crane and D. L Iglehart. “*Simulating Stable Stochastic Systems, I: General Multi-Server Queues*”. Vol. Journal of the Association of Computing Machinery, 21, 103-113. 1975.
- [49] B. D Ripley. “*Stochastic Simulation*”. Vol. New York: Wiley. 1987.
- [50] G. L. Jones and J. P. Hobert. “*Honest Exploration of Intractable Probability Distributions via Markov Chain Monte Carlo*”. Vol. Statistical Science, 16, 312-334. 2001.
- [51] Luke Tierney Per Mykland and Bin Yu. “*Regeneration in Markov Chain Samplers*”. Vol. Journal of the American Statistical Association, Vol. 90, No. 429 pp. 233-241. 1995. [http://www.jstor.org/stable/2291148..](https://www.jstor.org/stable/2291148..)